2014

CLOGGING OF FINE SEDIMENT WITHIN GRAVEL SUBSTRATES: MACRO-ANALYSIS AND MOMENTUM-IMPULSE MODEL

Davis Huston
University of Kentucky, davis.huston@stantec.com

STUDENT AGREEMENT:

I represent that my thesis or dissertation and abstract are my original work. Proper attribution has been given to all outside sources. I understand that I am solely responsible for obtaining any needed copyright permissions. I have obtained needed written permission statement(s) from the owner(s) of each third-party copyrighted matter to be included in my work, allowing electronic distribution (if such use is not permitted by the fair use doctrine) which will be submitted to UKnowledge as Additional File.

I hereby grant to The University of Kentucky and its agents the irrevocable, non-exclusive, and royalty-free license to archive and make accessible my work in whole or in part in all forms of media, now or hereafter known. I agree that the document mentioned above may be made available immediately for worldwide access unless an embargo applies.

I retain all other ownership rights to the copyright of my work. I also retain the right to use in future works (such as articles or books) all or part of my work. I understand that I am free to register the copyright to my work.

REVIEW, APPROVAL AND ACCEPTANCE

The document mentioned above has been reviewed and accepted by the student's advisor, on behalf of the advisory committee, and by the Director of Graduate Studies (DGS), on behalf of the program; we verify that this is the final, approved version of the student's thesis including all changes required by the advisory committee. The undersigned agree to abide by the statements above.

Davis Huston, Student

Dr. James Fox, Major Professor

Dr. Yi-Tin Wang, Director of Graduate Studies

CLOGGING OF FINE SEDIMENT WITIHIN GRAVEL SUBSTRATES: MACRO-ANALYSIS AND MOMENTUM-IMPULSE MODEL

THESIS

A thesis submitted in partial fulfillment of the requirements for the degree of Master of Science in Civil Engineering in the College of Engineering at the University of Kentucky

By

Davis Huston

Lexington, Kentucky

Director: Dr. James Fox, Professor of Civil Engineering

Lexington, Kentucky

2014

ABSTRACT OF THESIS

CLOGGING OF FINE SEDIMENT WITIHIN GRAVEL SUBSTRATES: MACRO-ANALYSIS AND MOMENTUM-IMPULSE MODEL

An understanding of the clogging of fine sediments within gravel substrates is advanced through the use of dimensional analysis and macro-analysis of clogging experiments in hydraulic flumes. Dimensional analysis is used to suggest that the dimensionless clogging depth can be collapsed using the original and adjusted bed-to-grain ratios, substrate porosity, roughness Reynolds number, and Peclet number. Macro-analysis followed by statistical analysis of 146 experimental test results of fine sediment deposition in gravel substrates suggests that the dimensionless clogging depth can be collapsed using the substrate porosity and roughness Reynolds number reflecting the processes of gravity settling and turbulence induced fluid pumping between substrate particles. In addition, a clear cutoff of fine sediment unimpeded static percolation and sediment clogging is found using the adjusted bed-to-grain ratio.

Thereafter, a physics-based approach is used to predict the clogging depth of fine sediment in gravel and in turn approve upon the preliminary findings in the empirical analysis. A momentum-impulse model that accounts for the critical impulse of a particle bridge is balanced with a fluid pulse resulting from turbulent pumping. The momentum-impulse model reduces the number of unknown parameters in the clogging problem and increases the model predictability as quantified using k-fold validation and model comparison with the empirical approach. A nomograph derived from applying the momentum-impulse model is provided herein, which will be useful for stream restoration

practitioners interested in estimating embeddedness. Also, prediction of the clogging profile is shown using the clogging depth predicted with the momentum-impulse model.

KEYWORDS: Sediment Transport, Streambed Clogging, Porosity, Fluid Pumping, Particle Bridging

Davis Huston

November 11, 2014

CLOGGING OF FINE SEDIMENT WITIHIN GRAVEL SUBSTRATES: MACRO-ANALYSIS AND MOMENTUM-IMPULSE MODEL

By

Davis Huston

James Fox, Ph.D.
Director of Thesis

Yi-Tin Wang, Ph.D.
Director of Graduate Studies

November 11, 2014
Date

AKNOWLEDGEMENTS

I would like to extend a special thanks to my advisor Dr. James Fox; you have been a tremendous mentor and have incited me to continue to strive for more. I am extremely grateful for your encouragement to grow as a research scientist, and your motivation and enthusiasm when I was near the end of my patience. Working under your guidance as an undergraduate research assistant changed the way I thought of civil engineering by introducing me to the field of water resources and sediment transport. Your advice and guidance has allowed me to improve as an engineer and set me on a career path that I love.

I would also like to thank my committee members Dr. Scott Yost and Dr. Carmen Agouridis for your brilliant insight and suggestions that continue to improve upon my research.

Furthermore, thanks to my family for their support and encouragement throughout my college career. Without you all none of this would have been possible.

TABLE OF CONTENTS

LIST OF TABLES

LIST OF FIGURES

Chapter 1: Introduction

Streambed clogging is the process of fine sediment infiltration and impingement within the pore spaces of streambeds. The clogging of fine fluvial sediment, defined as fine sands for our research, in a gravel bed substrate for hydraulically rough turbulent flow in open channels remains an important process to study due to its numerous environmental impacts. Excessive infiltration of fine sediment into gravel beds can have deleterious effects on benthic organisms. The clogging of salmonid redds can smother eggs due to a reduction in re-oxygenating intra-gravel flows (Wood and Armitage, 1997). Macroinvertibrates use the substrate for deposition of eggs, feeding, and shelter. The clogging of substrate pores reduces the trapping of nutrients, limits the availability of oxygen, and decreases the amount of accessible pore spaces for macroinvertibrates (Bo et al., 2007). Due to the large surface area associated with fine sediment, fine sediment can act as a sink for contaminants. The flux of fine sediment into porous gravel should be considered in assessment of contaminant transport (Krou et al., 2006). Deposition of fine sediments in streambed substrates can also have a significant effect on aquatic ecosystem stability, hyporheic exchange of nutrients, and ecosystem carbon budgets (Ford and Fox, 2014). The process of fine sediment clogging in a gravel streambed is characterized by the deposition of fine particles to the top layer of the bed and intrusion of the fine particles into the pore spaces of the gravel substrate (see Figure 1). Deposition of fines to the water-sediment interface occurs when the downward gravity and fluid pumping forces acting on fine particles exceeds the force associated with upward turbulent ejections (Fries and Trowbridge, 2003). Upon transport below the water-sediment interface, the fine particles can infiltrate to the sediment intrusion depth, decelerate, and then coalesce to form stable multi-particle bridges across pores in the gravel substrate (Sakthivadivel and Einstein, 1970). We refer to this relatively deep sediment intrusion depth with stable multi-particle bridges as the maximum clogging depth, Z_C (see Figure 1), and the focus of this thesis is prediction of Z_C. Experimental observations of gravels clogged with fine sand has shown that the fraction of sand deposit is maximized near the water-sediment interface referred to as a ‘surface seal’ and decreases exponentially to Z_C (Dermisis and Papanicolaou, 2014).

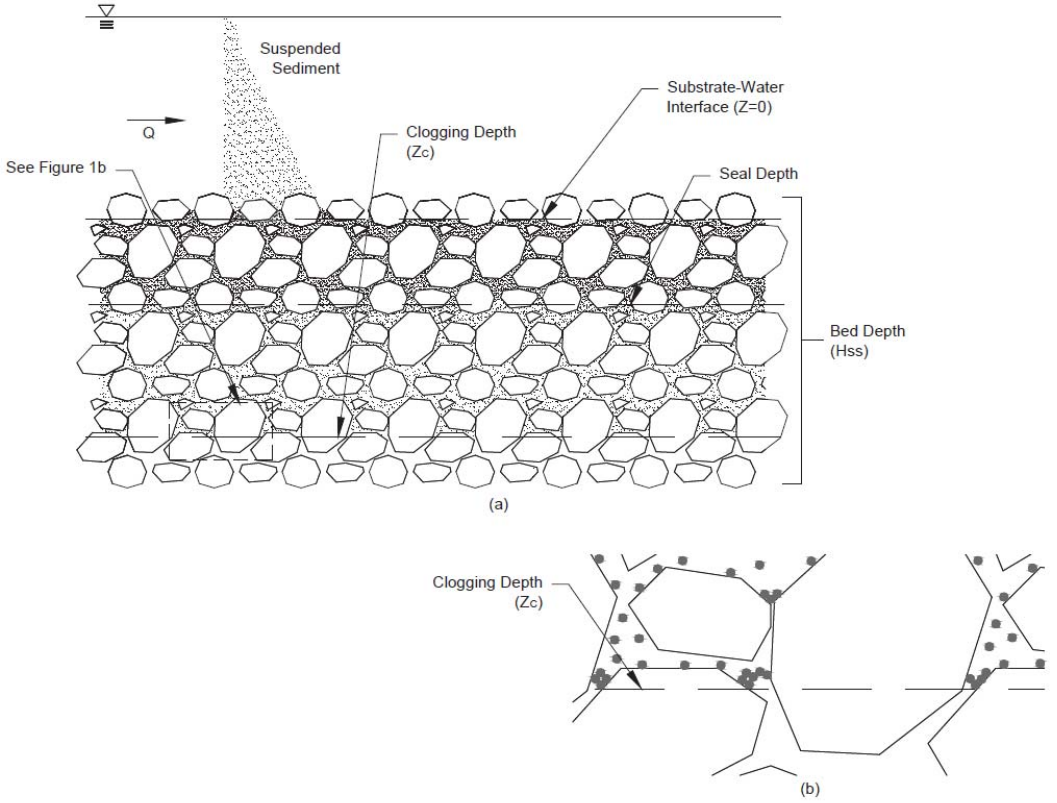

Figure 1. Definition sketch of the clogging process showing (a) the fine sediment distribution with depth in the gravel and (b) multi-particle bridging at Z_C.

This thesis will explore the physical processes governing the clogging of gravel substrates by fine sediment through a meta-analysis and dimensional analysis; then develop a physics-based model to predict the clogging depth of fine sediment in gravel. Chapter 2 advances the understanding of the clogging of fine sediments within gravel substrates through use of dimensional analysis and macro-analysis of previously-conducted clogging experiments in hydraulic flumes. Dimensional analysis via the Buckingham Pi Theorem is used to suggest that the dimensionless clogging depth can be potentially collapsed using the original and adjusted bed-to-grain ratios, i.e., ratio of substrate diameter to fine sediment diameter, substrate porosity, roughness Reynolds number and Peclet number. Macro-analysis followed by statistical analysis is performed using 10 previously published studies that include a total of 146 different test conditions reporting noncohesive, fine sediment clogging or deposition in porous gravel-beds with

hydraulically rough turbulent open channel flow. Thereafter, an empirical model is developed that predicts Z_c, which is then used to estimate the clogging profile for fine sands in gravel substrate for the datasets. Chapter 3 develops a momentum-impulse model that accounts for the critical impulse of a particle bridge that is balanced with a fluid pulse resulting from turbulent pumping. The momentum-impulse model is presented and applied for predicting the clogging depth of fine sand in gravel streambeds overlain by turbulent open channel flow. The model was tested against the literature-derived database of clogging depth detailed in Chapter 2. A nomograph derived from running the momentum-impulse model is provided herein, which will be useful for stream restoration practitioners interested in estimating embeddedness. Furthermore, we show prediction of the clogging profile using our clogging depth predicted with the momentum-impulse model.

Chapter 2: Dimensional Analysis and Macro-Analysis of Experiments in Hydraulic Flumes

2.1 SUMMARY

An understanding of the clogging of fine sediments within gravel substrates is advanced through use of dimensional analysis and macro-analysis of previously-conducted clogging experiments in hydraulic flumes. Dimensional analysis via the Buckingham Pi Theorem is used to suggest that the dimensionless clogging depth can be potentially collapsed using the original and adjusted bed-to-grain ratios, i.e., ratio of substrate diameter to fine sediment diameter, substrate porosity, roughness Reynolds number and Peclet number. Macro-analysis followed by statistical analysis is performed using 10 previously published studies that include a total of 146 different test conditions reporting noncohesive, fine sediment clogging or deposition in porous gravel-beds with hydraulically rough turbulent open channel flow. Results suggest that the adjusted bed-to-grain ratio is a reliable predictor of the initiation of clogging with clogging occurring below 27 for the fine fluvial sediment clogging in a gravel bed substrate for hydraulically rough turbulent flow flumes considered. The original and adjusted bed-to-grain ratios show little influence on the depth of clogging once the lower threshold for bed filling is reached. Contrary to conventional wisdom, the bed-to-grain ratio is not used to predict the maximum depth of clogging. Rather, results suggest that the dimensionless clogging depth can be collapsed using the substrate porosity and roughness Reynolds number reflecting the impact of the pore water velocity distribution on the dispersion of fine sediment into the gravel substrate. The clogging depth results are used to estimate the clogging profile for fine sands in gravel substrate for the datasets.

2.2 INTRODUCTION

In depth study of the clogging problem has tended to focus on experimental investigation in the laboratory and has undergone a number of developmental stages in research. Einstein (1968) pioneered the first fine sediment infiltration into gravel bed experiments in a recirculating, laboratory flume and found fine sediment infiltrates the

bed to unlimited clogging depth ($Z_C=\infty$) and proceeds to fill the gravel interstices upward. A second stage of research included a number of clogging studies under a range of sediment conditions which found that sediment can infiltrate to a finite depth ($Z_C<\infty$), and the occurrence of a finite Z_C was attributed to the bed-to-grain ratio, defined as the ratio of the substrate gravel diameter to the fine sediment diameter (Beschta and Jackson, 1979; Carling, 1984; Diplas and Parker, 1985). A third stage of research has focused on detailed observation and modeling of the profile for the fine sediment deposit shown in Figure 1 for a range of hydraulic and sediment conditions (Wooster et al., 2008; Cui et al., 2008; Gibson et al., 2008; Gibson et al., 2010; Gibson et al., 2011; Dermisis and Papanicolaou, 2014).

The previous mentioned studies have provided labor- and time-intensive experimental data of the clogging problem, and at the same time, advanced our understanding of the process to arrive at the clogging profile shown in Figure 1. However, critique of the literature suggests that there are a number of advancements needed for understanding and predicting the clogging of fine sediment in gravel beds, especially with emphasis on prediction of Z_C. First, a threshold for clogging (i.e., $Z_C=\infty$ or $Z_C<\infty$) has not be well established for the clogging of fine sand in gravel substrate overlain by hydraulically rough open channel flow. Taken together, the prior experiments reinforce the control of the bed-to-grain ratio on the initiation of clogging and minimize the control of parameters such as the suspended sediment load and bulk Froude number upon an infinite or finite Z_C (Beschta and Jackson, 1979; Carling, 1984; Diplas and Parker, 1985; Wooster et al., 2008; Gibson et al., 2008; Gibson et al., 2010; Gibson et al., 2011; Kuhnle et al., 2013). A threshold for clogging remains unclear; macro-analysis of the prior studies has not been performed in an effort to find some generality of the previously published results of fine sediment clogging in gravel substrate. Further, detailed discussion and analyses of the fundamental process likely responsible for the onset of clogging, i.e., multi-particle bridging within gravel pore spaces, has not been provided in the literature.

A second advancement needed for the clogging process is prediction of Z_C based on hydraulic and sediment parameters for conditions in which the maximum clogging depth is finite ($Z_C<\infty$). It is now recognized that the location of Z_C is established temporarily early in the sediment intrusion and clogging process prior to establishment of the exponential fine sediment profile associated with filling up and sealing of gravel pore spaces near the water-sediment interface (Gibson et al., 2011). The relatively early onset of Z_C suggests a conceptual model for clogging that includes the downward dispersion of fine particles at the beginning stages of the process likely as a function of the pore water velocity distribution for the unclogged gravel pores. Thereafter, the fine sediment front progresses and particles continue to infiltrate the gravel pores above the location of Z_C, which in turn dampens the pore water velocity distribution throughout the gravels and allows bridging to occur closer and closer to the water-sediment interface. Eventually, progression of the sediment front causes the upper gravel layers to be completely clogged, i.e., sealed, preventing fine particles from passing to the lower layers and effectively stopping the clogging process to produce the observed exponential profile. Our conceptual model for the temporarily early onset of clogging enabled us to hypothesize that Z_C will show dependence upon parameters impacting the pore water velocity distribution such as the friction velocity and roughness at the water-sediment interface and the porosity and permeability of the substrate.

The objective of this chapter was to advance our understanding of the clogging of fine sediments within gravel substrates through use of dimensional analysis and macro-analysis of previously-conducted clogging experiments in hydraulic flumes. After conducting a dimensional analysis of the parameters controlling clogging, we performed a macro-analysis of 10 studies that included a total of 146 different test conditions reporting fine sands and silts clogging or deposited in porous gravel-beds with hydraulically rough turbulent open channel flow. Through this analysis, this thesis provides two major advancements to the clogging problem. First, an adjusted bed-to-grain ratio provides a clear cutoff of the threshold of clogging under fine sediment and gravel substrate conditions for the 146 tests considered. Second, a new dimensional analysis provides a dimensionless clogging depth that is predictable using substrate

porosity and roughness Reynolds number, which in turn reflect the processes of fluid pumping in porous gravel bed and the formation of multi-particle bridges at Z_C.

2.3 DIMENSIONAL ANALYSIS

In this section, we provide results of dimensional analysis to arrive at a dimensionless number for Z_C as well as dimensionless parameters that might be useful in: (i) predicting a threshold for clogging for $Z_C=\infty$ or $Z_C<\infty$; and (ii) predicting Z_C for conditions in which $Z_C<\infty$. To this end, clogging of fine sediment within porous gravel substrate is hypothesized to be a function of both the pore space geometry at which the multi-particle bridging within gravel pore space will occur and the pore space velocity responsible for transporting fine sediments deeper into the bed.

Multi-particle bridging within gravel pore space will be expected to show dependence upon fine sediment and gravel substrate physical characteristics including d_{fs} and d_{ss} defined as the geometric mean diameter of the fine suspended sediment and substrate sediment, respectively. The influence of d_{fs} and d_{ss} upon multi-particle bridge formation has been well established in fundamental particle bridge studies (Valdes and Santamarina, 2008), in more general filtration and porous media transport studies (McDowell-Boyer et al., 1986; Wu and Huang, 2000; Fries and Trowbridge, 2003), and empirical clogging studies specific to fine sands in gravel substrate overlain by hydraulically rough open channel flow (Beschta and Jackson, 1979; Carling, 1984; Diplas and Parker, 1985; Wooster et al., 2008; Gibson et al., 2008; Gibson et al., 2010; Gibson et al., 2001; Kuhnle et al., 2013). A secondary parameter of the gravel substrate physical characteristics expected to show dependence upon bridging was the geometric standard deviation of the substrate sediment (σ_{ss}). As σ_{ss} increases, the bed material becomes more well-graded, the potential exists for macropores to be filled with smaller particles within the substrate mixture and thus reduce the substrate porosity and thus pore size for bridging (Sohn and Moreland, 1968; Dexter and Tanner, 1972; Wakeman, 1975).

The dependence of Z_C upon the pore space velocity responsible for dispersing and transporting fine sediments deeper into the gravel bed is hypothesized to be significant. While experimental results of the pore water velocity distribution have not been reported for conditions of the previously reported clogging studies, a number of parameters impacting the pore water velocity distribution have been reported in the turbulent open channel flow literature. The pore water velocity has long been considered a function of the fluid shear velocity (u_*) at the fluid-substrate interface (Nagaoka and Ohgaki. 1990; Shimizu et al., 1990), which reflects the pulsation of turbulent eddies at the streambed. Furthermore, the roughness height (k_s) of substrate sediment protruding into the flow field has now been reported to impact the turbulent structure and fluid transport to the subsurface associated with turbulent diffusion on the lee side of protruding grains (Reidenbach et al., 2010); and isolated large roughness elements have been reported to impact the fine sediment intrusion depth due to downwelling at the stoss (Dermisis and Papanicolaou, 2014). Within the pore spaces of the gravel substrate, the dissipation of the pore water velocity distribution to Darcian velocity is expected to be a function of the pore space volume and the fluid properties. The former can be expressed using the porosity of the substrate sediment (φ) or specifically the streambed permeability (K) which impact the subsurface velocity (Wu and Huang, 2000) while the latter are reflected in the properties of fluid viscosity (μ) and density (ρ).

With the above discussion of mechanisms and governing parameters in mind, Z_c was expected to potentially show dependence upon the following sediment and fluid variables

$$Z_c = fn\left(d_{fs}, d_{ss}, \sigma_{ss}, \varphi, K, k_s, u_*, \rho, \mu\right) . \quad (1)$$

Equation (1) provides a functional dependence between Z_C with emphasis on predicting a threshold for clogging ($Z_C=\infty$ or $Z_C<\infty$) and predicting Z_C for conditions in which $Z_C<\infty$. As previously mentioned, a number studies have suggested the importance of the substrate median particle size and fine sediment median particle size, or bed-to-grain ratio, $\frac{d_{ss}}{d_{fs}}$, as a parameter controlling the threshold of clogging mechanism (Beschta and Jackson, 1979; Carling, 1984; Diplas and Parker, 1985; Wooster et al., 2008; Gibson et

al., 2008; Gibson et al., 2010; Gibson et al., 2001; Kuhnle et al., 2013). More specifically, it has been suggested that $\frac{d_{ss}}{d_{fs}}$ is a potential metric for predicting the initiation of clogging where an upper threshold of $\frac{d_{ss}}{d_{fs}}$ exists at which fine sediment passes through the substrate pores. This non-clogged scenarios is referred to as transport *via* unimpeded static percolation and under this mechanism intra-gravel pore spaces are sufficient to allow fine sediment to fall between bed clasts to the bottom of the bed substrate (Sakthivadivel and Einstein, 1970; Gibson et al., 2008; Gibson et al., 2010). Various studies have reported threshold values for separation of clogging and unimpeded static percolation predicted with $\frac{d_{ss}}{d_{fs}}$. For example, Sakthivadivel and Einstein (1970) suggest that for $\frac{d_{ss}}{d_{fs}} > 20$ minimal clogging of porous media exists. Gibson et al. (2008, 2010) suggests that for $\frac{d_{ss}^{15}}{d_{fs}^{85}} > 15.4$, unimpeded static percolation will occur, where d_{ss}^{15} is the diameter of substrate of which 15% is finer than and d_{fs}^{85} is the diameter of fine sediment of which 85% is finer than. Macro-analysis of many studies might provide some generality to the threshold $\frac{d_{ss}}{d_{fs}}$ value for clogging. But also, we suggest that adjusting the bed-to-grain ratio to include the influence of σ_{ss} as $\frac{d_{ss}}{d_{fs}\sigma_{ss}}$ might improve our prediction of the initiation of clogging in order to account for the potential of macropores to be filled with smaller particles within the substrate mixture and thus reduce the size of the pore spaces. Due to the potential influence of σ_{ss}, we test both $\frac{d_{ss}}{d_{fs}}$ and $\frac{d_{ss}}{d_{fs}\sigma_{ss}}$ for their ability to predict clogging.

Using the above arguments, Equation (1) is updated as

$$Z_c = fn\left(\frac{d_{ss}}{d_{fs}}, \frac{d_{ss}}{d_{fs},\sigma_{ss}}, \varphi, K, k_s, u_*, \rho, \mu\right), \quad (2)$$

where $\frac{d_{ss}}{d_{fs}}$, $\frac{d_{ss}}{d_{fs},\sigma_{ss}}$ and φ are dimensionless. We performed dimensional analysis *via* the Buckingham PI Theorem using the remaining variables with dimensions in Equation (2)

and treated u_*, ρ and μ as repeating variables to produce five dimensionless parameters as follows

$$\frac{Z_C u_* \rho}{\mu} = fn\left(\frac{d_{ss}}{d_{fs}\sigma_{ss}}, \varphi, \ \frac{k_S u_* \rho}{\mu}, \frac{K^{0.5} u_* \rho}{\mu}\right). \quad (3)$$

Equation (3) shows the functional dependence of the newly defined dimensionless clogging depth (Z_C^*), defined as

$$Z_C^* = \frac{Z_C u_* \rho}{\mu}, \quad (4)$$

upon the bed-to-grain ratio, adjusted bed-to-grain ratio, bed porosity, and the recognizable roughness Reynolds number, defined as

$$Re^* = \frac{k_S u_* \rho}{\mu}, \quad (5)$$

and the recognizable Peclet number, defined as

$$Re_K = \frac{K^{0.5} u_* \rho}{\mu}. \quad (6)$$

Equation (3) can be equivalently and concisely written using the symbols for dimensionless parameters in Equations (4), (5) and (6) as

$$Z_C^* = fn\left(\frac{d_{ss}}{d_{fs}}, \frac{d_{ss}}{d_{fs},\sigma_{ss}}, \varphi, Re^*, Re_K\right). \quad (7)$$

The result in Equation (7) tends to agree well with the literature surrounding solute and fine sediment transport within porous gravel-beds. For example, the bed-to-grain ratio has been commonly used in previous clogging studies, the porosity is well recognized as controlling in solute transfer, and both the roughness Reynolds number and Peclet number are commonly included in macro-analysis of filtration processes and

solute transfer (Fries and Trowbridge, 2003; O'Conner and Harvey, 2008; Wooster et al., 2008). In this manner, the dimensionless numbers in Equation (7) offered the potential of predicting a threshold for clogging ($Z_C=\infty$ or $Z_C<\infty$) and predicting Z_C for conditions in which $Z_C<\infty$ due to the parameters ability to capture mechanisms of the multi-particle bridging within gravel pore space and the pore space velocity responsible for dispersing fine sediments deeper into the bed. Our interest was to test the ability of the dimensionless parameters in Equation (7) to provide any generality and thus collapse reported measurements of Z_C^*. We performed macro-analysis of existing reported values for clogging depth and statistical analysis to meet this goal.

2.4 MACRO-ANALYSIS AND STATISTICAL ANALYSIS

In order to test the results of the dimensional analysis in Equation (7) for predicting a threshold for clogging for $Z_C=\infty$ or $Z_C<\infty$ and predicting Z_C for conditions in which $Z_C<\infty$, we performed a macro-analysis and compiled experimental results of previous clogging studies. Our focus was to include studies that allow inference of processes including multi-particle bridging within pore spaces and the turbulence and subsurface geometry's impact on the pore water velocity distribution that in turn result in the location of Z_C. To this end, we chose published studies with the following characteristics: (i) experiments in laboratory hydraulic flumes where hydraulic and sediment conditions can be highly controlled and the occurrence of Z_C and its approximate location is measureable; (ii) clogging experiments defined as fine sand intruding into porous gravel substrate initially void of fine material which would allow multi-particle bridges to be formed within gravels or unimpeded static percolation to the bottom of the flumes; (iii) hydraulically rough turbulent open channel flow over gravel bed which would be expected to produce turbulent structure in the vicinity of protruding roughness elements that could enhance fine sediment dispersion into the bed; (iv) open channel flow ranging from subcritical to critical conditions that will be free of pronounced surface waves that might penetrate fine sand deeper into the gravel bed and further complicate the process; and (v) substrate conditions in which gravels are

immovable which could cause secondary settling of fines deeper into the gravel substrate and confound the initial Z_C hypothesized to occur due to fine sand dispersion associated with the pore water velocity distribution.

With the above hydraulic and sediment conditions in mind, our macro-analysis included 10 previously published studies. Table 1 compiles 146 test conditions for 10 studies that report results of clogging and unimpeded static percolation of fine fluvial sediment in a gravel bed substrate for hydraulically rough turbulent flow in open channel flumes, including Einstein (1968), Beschta and Jackson (1979), Dhamotharan and Shirazi (1980), Carling (1984), Diplas and Parker (1985), Wooster et al. (2008), Gibson et al. (2008), Gibson et al. (2010), Gibson et al. (2011) and Kuhnle et al. (2013).

Our macro-analysis was performed in two stages. First, the 146 test conditions for the 10 studies were used to predict a threshold for clogging for $Z_C=\infty$ or $Z_C<\infty$. Second, experimental tests for which $Z_C<\infty$ were used to predict Z_C with the dimensionless parameters. In the second stage, the studies of Einstein (1968), Carling (1984) and Kuhnle et al. (2013) are not included because $Z_C=\infty$ for all of the experimental tests reported in these papers. Also, the results of Beschta and Jackson (1979) are not included in the second stage of investigation because their results reported only a sealing depth and did not provide enough information to estimate Z_C from the results.

Table 1 includes values for d_{fs}, d_{ss}, σ_{ss}, φ, K, k_s, u_*, ν, Z_C, Fr, Re^* and Re_K compiled from the 10 published studies (see Appendices). Fluid used in all studies was water in hydraulic flumes. Fine sediment in all studies were sand-sized grains with the exception of Einstein's (1968) study which used silt-sized grains. Gravel-beds ranged in size from approximately 2 to 90 mm. The majority of the studies were subcritical flow with some studies at or near critical conditions. All studies were hydraulically rough as indicated by Re^* greater than 100. Many of the parameters compiled in Table 1 were reported in the papers, however, some parameter were not directly reported and were approximated as follows. The standard deviation of the substrate gravel diameters was estimated using the reported grain size distribution curves as

$$\sigma_{ss} = \sqrt{\frac{d_{ss}^{85}}{d_{ss}^{15}}} \quad . \tag{8}$$

where d_{ss}^{85} and d_{ss}^{15} are the diameters of substrate sediment of which 85% and 15% are finer, respectively. The bed roughness height was approximated as d_{ss}^{85}, which has been shown both experimentally and semi-theoretically to be responsible for dominant roughness conditions in gravel bed flumes and rivers (Belcher and Fox, 2011). Approximation of the shear velocity was calculated as

$$u_* = \sqrt{gHS} \quad . \tag{9}$$

where g is gravitational acceleration, H is gravel bed depth, and S is the bed slope. As needed, gravel bed porosity was estimated using the empirical equation provided by Wooster et al. (2008) which was developed for gravel-beds with 0.004 m < d_{ss} < 0.018 m as

$$\varphi = 0.621\sigma_{ss}^{-0.659} \quad . \tag{10}$$

While some previous researchers provided a porosity value for their substrates, they did not indicate how these porosities were determined. Bed permeability was estimated using the widely known Kozeny-Carmen equation (e.g., Chapuis and Aubertin, 2003) as

$$K = 0.0056 d_{ss}^2 \frac{\varphi^3}{(1-\varphi)^2} \quad . \tag{11}$$

Dhamotharan et al. (1980), Wooster et al. (2008) and Gibson et al. (2008, 2010 and 2011) provided infiltrating fine sediment profiles. In order to estimate Z_C for the datasets, a linear regression line via least squares error minimization was optimized to each dataset in these papers, and the location where the linear regression line crossed the depth axis was used to approximate Z_C. While it is recognized that the clogging profile has been observed to reflect an exponential decay, the linear regression approach was justifiable because we found that the linear regression technique provided a repeatable,

quantitative method for predicting Z_C at near zero fine sand fractions that remained constant with greater depths. For the Diplas and Parker (1985) study, the maximum sediment intrusion depth was used as an estimate of Z_C. Beschta and Jackson (1979) stated that the seal depth occurred in the top 5 cm for their lowest Froude number condition, the top of the 5-10 cm layer for their moderate Froude number condition, and deeper intrusion into the 5-10 cm layer occurring for their highest Froude number condition. Average seal depth for these conditions was estimated as 3, 6 and 9 cm corresponding to the low, moderate and high Froude numbers. Because Beschta and Jackson (1979) only reported a seal depth, their datasets were not used in the dimensionless Z_C analyses.

The relationships between dimensionless clogging depth and the potential explanatory parameters were tested and statistically analyzed to determine dependence. Each of the dimensionless parameters were individually plotted against dimensionless clogging depth and a linear regression analysis via least squares error minimization was performed. This process was performed a second time with the exclusion of several leverage points, which is further discussed in the results. Thereafter, combinations of dimensionless parameters were iterated, optimized and statistically analyzed in order to provide the best collapse of dimensionless clogging depth.

2.5 RESULTS

After analyzing the 10 studies and 146 experimental tests, we found a clear cutoff between the initiation of clogging ($Z_C<\infty$) and unimpeded static percolation of fine sediments to the bottom of the experimental flumes ($Z_C=\infty$). $\frac{d_{ss}}{d_{fs}\sigma_{ss}}$ separated the experimental tests with a threshold value of 27 (see Figure 2). Experimental tests in which the adjusted bed-to-grain ratio was greater than 27 resulted in unimpeded static percolation of fine sediments to the bottom of the experimental flumes ($Z_C=\infty$). Experimental tests in which the adjusted bed-to-grain ratio was less than 27 resulted in a fine sediment clogging at some depth above the bottom of the experimental flume

($Z_C<\infty$). Similar results were found for use of the traditional bed-to-grain ratio, $\frac{d_{ss}}{d_{fs}}$. The $\frac{d_{ss}}{d_{fs}}$ separated the experimental tests with a threshold value of 37. Experimental tests in which the bed-to-grain ratio was greater than 37 resulted in static percolation to the bottom of the flume ($Z_C=\infty$). Clogging occurred ($Z_C<\infty$) when the bed-to-grain was less than 37. Two tests performed by Gibson et al. (2010) had $\frac{d_{ss}}{d_{fs}}$ equal to 46 suggesting unimpeded static percolation; however, the experiments resulted in clogging and thus showed a lack of prediction for the bed-to-grain ratio for these conditions. For this reason, the adjusted bed-to-grain ratio is suggested as a better predictor of the threshold of clogging as compared to the traditional bed-to-grain ratio for the experimental conditions investigated in this macro-analysis.

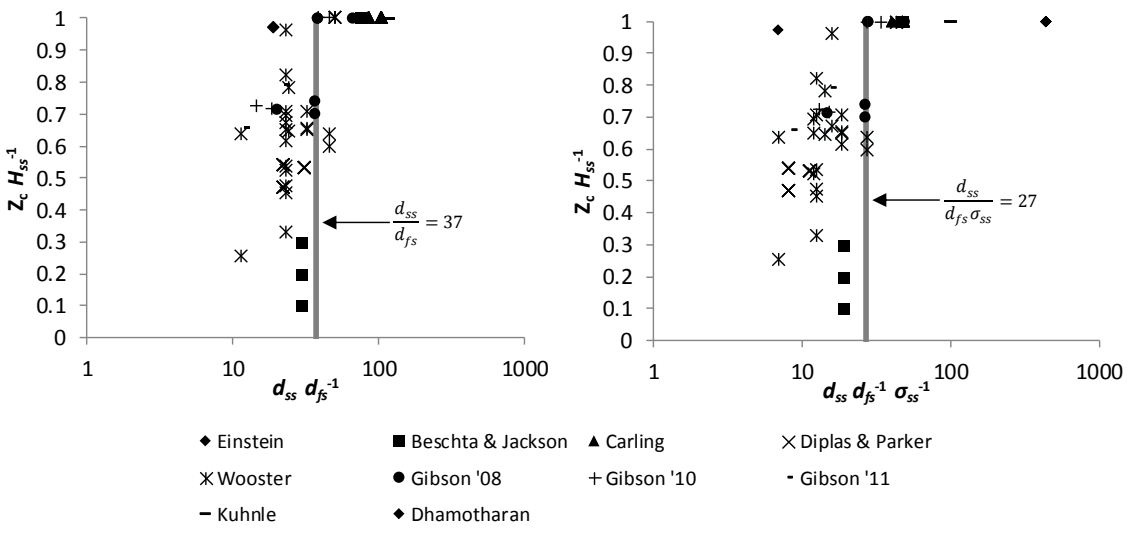

(a)

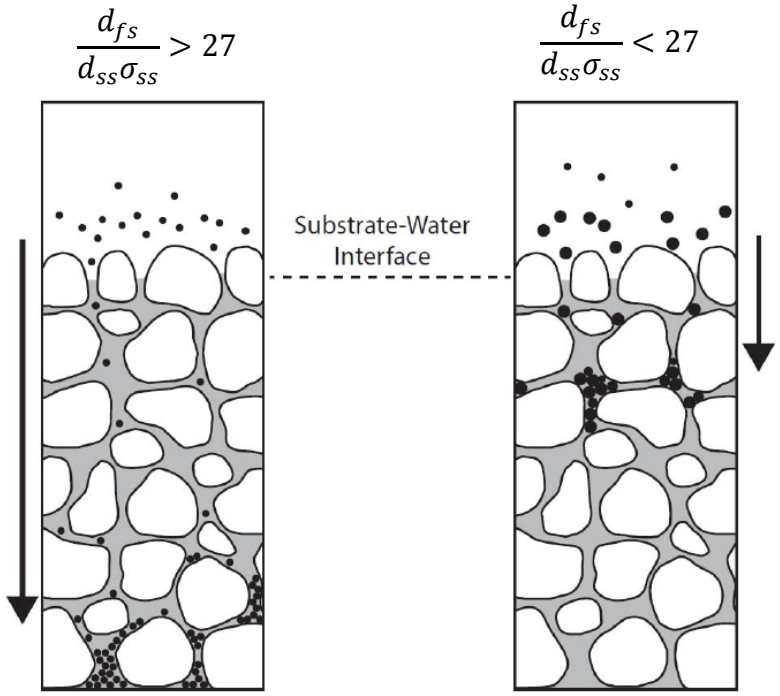

(b) (c)

Figure 2. Figure 2a shows comparison traditional bed-to-grain ratio and adjusted bed-to-grain ratio. Figure 2b shows unimpeded static percolation while figure 2c on the right shows particle bridging.

We removed the results defined as unimpeded static percolation and then statistically analyzed the remaining results from the experimental tests where clogging did occur in order to test the ability of the dimensionless parameters in Equation (7) to provide any

generality and thus collapse reported measurements of Z_C^*. Linear regression using the individual dimensionless parameters as predictors and Z_C^* as the response variable showed that φ was the single best predictor of Z_C^* followed by Re_K and Re^* as good predictors (see Figure 3 and Table 2). Empirical Z_C^* for the single predictors were optimized as

$$Z_C^* = 5.8 \times 10^4 \varphi + 1.8 \times 10^4, \quad (12)$$

$$Z_C^* = 6.0\, Re^* + 398 \text{ and} \quad (13)$$

$$Z_C^* = 220\, Re_K + 1243\,. \quad (14)$$

where R^2 was equal to 0.72, 0.65 and 0.67, respectively, for the macro-analysis in Figure 3a, b and c. $\frac{d_{ss}}{d_{fs}\sigma_{ss}}$ and $\frac{d_{ss}}{d_{fs}}$ were the weakest predictors (see Table 2). Through multi-parameter statistical analysis, we found that coupling φ and Re^* produced the best collapse of the experimental tests in prediction of Z_C^* (see Figure 3d), and the coupled parameter indicates statistical significance (see Table 2). The two parameter equation for Z_C^* was optimized as

$$Z_C^* = 2.3 \times 10^4\, \varphi^{0.6} Re^{*0.1} + 2.0 \times 10^4\,, \quad (15)$$

where R^2 was equal to 0.85 for the macro-analysis in Figure 3d.

Table 1. Z_C^* statistical dependence upon single and multiple dimensionless parameters.

Parameter	R^2	p-Value	
		Slope	R^2
$d_{ss}d_{fs}^{-1}$	0.0004	0.449	0.999
$d_{ss}d_{fs}^{-1}\sigma_{ss}^{-1}$	0.23	0.003	0.464
Re^*	0.65	$<10^{-4}$	0.119
Re_K	0.67	$<10^{-4}$	0.107
φ	0.72	$<10^{-4}$	0.079
$\varphi^{0.6}Re^{*0.1}$	0.85	$<10^{-4}$	0.027

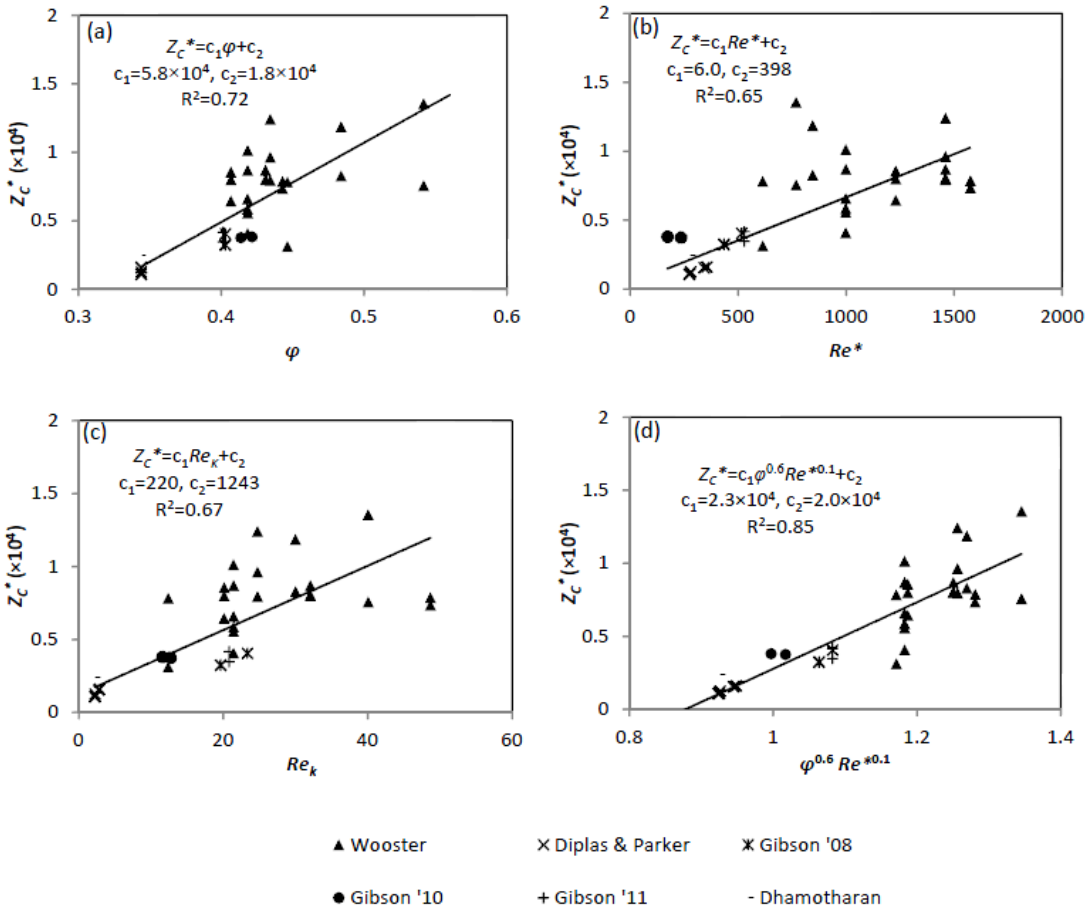

Figure 3. Dimensionless clogging depth collapse using dimensionless parameters. (a.) shows the linear relationship of the dimensionless clogging depth plotted with: (a) porosity, (b) the Reynolds roughness number, (c) the Peclet number, and (d) the optimized dimensionless clogging parameter.

2.6 DISCUSSION

The results in Figure 2 suggest the adjusted bed-to-grain ratio as a threshold parameter for initiation of clogging of fine sand within gravel substrate for hydraulically rough open channel flow over a gravel-bed. Our results suggest that fine sand transport over gravel streambeds with $\frac{d_{ss}}{d_{fs}\sigma_{ss}}$ less than 27 will experience clogging at some depth leaving the lower extents of the gravel substrate void of sand while stream conditions with $\frac{d_{ss}}{d_{fs}\sigma_{ss}}$ greater than 27 will experience fine sand transport to the lower extent of the gravel substrate and filling available void spaces. The fundamental reason that the adjusted bed-to-grain ratio is a threshold for clogging can be explained by the fact that sand particles form multi-particle bridges within the pore spaces of the gravel substrate (Sakthivadivel and Einstein, 1970). When $\frac{d_{ss}}{d_{fs}\sigma_{ss}}$ is large, i.e., greater than 27 for the fine sand and gravel substrate conditions of this study, bridges do not form and unimpeded static percolation of sand particles occurs to the bottom of the experimental flumes (Gibson et al., 2010).

Applicability of the threshold for clogging found in this macro-analysis of experimental results relies on the ability of the laboratory streambed conditions to fully allow clogging. Specifically, one may ask: would clogging have eventually occurred if the gravel substrate in the flume was much deeper? We argue that the experiments with $\frac{d_{ss}}{d_{fs}\sigma_{ss}} > 27$ would not have clogged with a deeper gravel streambed depth due to the fact that the pore spaces between gravel particles would have been too large to allow the building of multi-particle bridges. In order to support this claim, we use the trigonometric Heron's Formula (see Figure 4) to estimate the pore size, d_o, between three gravel particles with unequal diameters, d_1, d_2 and d_3, as

$$[d_1 d_2 d_3 (d_1 + d_2 + d_3)]^{0.5} = [d_1 d_2 d_o (d_1 + d_2 + d_o)]^{0.5} + [d_1 d_3 d_o (d_1 + d_3 + d_o)]^{0.5} + [d_2 d_3 d_o (d_2 + d_3 + d_o)]^{0.5} \quad \text{(Lauck, 1991).} \tag{16}$$

The pore diameter in Equation (16) can be compared with the fine sediment diameter, d_{fs}, to calculate the pore space diameter to fine sediment ratio, d_o:d_{fs}, which has been used in a number of fundamental particle bridging studies. d_o:d_{fs} was estimated for all fine sediment and gravel substrate test conditions reported in Table 1. For each test condition, the implicit Heron's Formula was solved for 1000 separate realizations based draws from the gravel bed particle size distributions and d_o:d_{fs} was calculated. Application of Heron's Formula assumes the gravel substrate particles can be treated as spheres to estimate d_o.

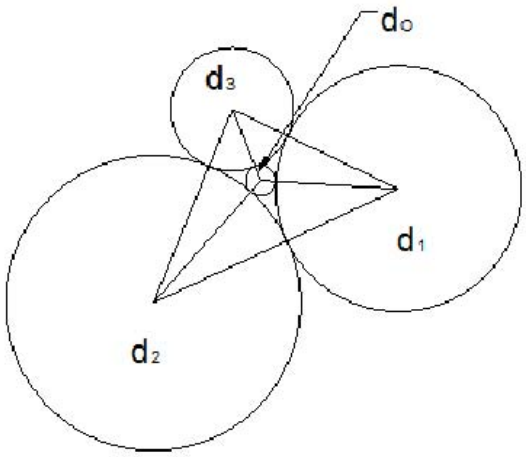

Heron's Formula: $\sqrt{(d_1 + d_2 + d_3)(d_1 d_2 d_3)} = \sqrt{(d_1 + d_2 + d_o)(d_1 d_2 d_o)} + \sqrt{(d_1 + d_3 + d_o)(d_1 d_2 d_o)} + \sqrt{(d_2 + d_3 + d_o)(d_2 d_3 d_o)}$

Figure 4. Heron's Formula for estimating the spherical pore size between three spheres with unequal diameters.

Figure 5 shows the pore throat analysis for the experimental tests in Table 1 macro-analysis. As can be seen, a cutoff occurs at d_o:d_{fs} equal to 5.5 in which experiments less than or equal to 5.5 had the occurrence of clogging in the gravel substrate. Most tests with d_o:d_{fs} greater than 5.5 did not have the occurrence of clogging and unimpeded static percolation of sand particles occurred to the

bottom of the experimental flumes. The cutoff d_o:d_{fs} result equal to 5.5 is remarkably similar with fundamental study performed by Valdes and Santamarina (2008), who found that stable multi-particle bridges will not form for pore spaces that are 4 to 5 times the fine particle diameter. The study by Valdes and Santamarina (2008) used perfectly spherical, uniform glass beads as the clogging material in spherical slots. Thus, the slight differences between d_o:d_{fs} equal to 5.5 in our approximation and d_o:d_{fs} to 4 to 5 in the Valdes and Santamarina (2008) study can be in part be attributed to the estimation of d_o. The actual pore size of a gravel bed framework can be particularly difficult to determine given the pore space size is dependent upon substrate particle size, shape, angularity and roughness; and it is recognized that streambed gravels are not perfectly spherical, smooth particles. Particle shape, angularity and roughness were not reported in the original papers considered in this study. The exception to the 5.5 cutoff value for d_o:d_{fs} was tests W-3 and W-23 by Wooster et al. (2008). Clogging did occur in the W-3 and W-23 tests even though d_o:d_{fs} was equal to 7.0 for both tests; thus showing disagreement with the 5.5 cutoff for d_o:d_{fs}. A possible explanation of the result is the gravel substrate size of the W-3 and W-23 test, which was equal to 16 mm and were the largest gravel substrate for which clogging occurred in the meta-analysis. Past work has shown that sphericity of gravel decreases as particle size increases (Peronius and Sweeting, 1985; Zou and Yu, 1996; Cho et al., 2006), and therefore perhaps the spherical assumption of Heron's Formula does not hold true for this condition. Nevertheless, in general the pore size analysis in Figure 5 supports the validity of the threshold for clogging results in Figure 2 and supports the idea that the gravel substrate in the experimental tests were in fact deep enough and clogging would likely have not occurred if the gravel substrate in the flume was much deeper. Our additional analysis supports the validity of the threshold for clogging as $\frac{d_{ss}}{d_{fs}\sigma_{ss}}$ equal to 27 for studies with fine sand within gravel substrate for hydraulically rough open channel flow over a gravel-bed with hydraulic and sediment conditions similar to those reported here.

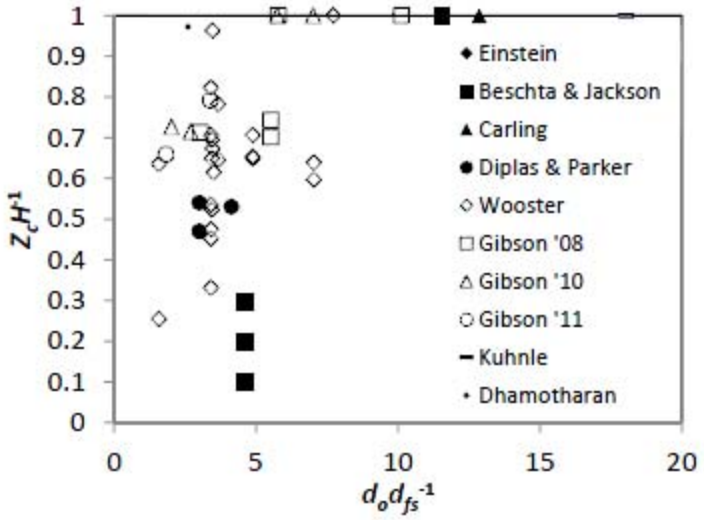

Figure 5. Threshold of clogging dependent upon the calculated pore space and fine sediment diameter.

Taken together, the Z_C^* results of the dimensionless predictor analysis (Re^*, φ, and Re_K in Figure 3) support our hypothesis that the maximum clogging depth (Z_C) is associated with the downward dispersion of fine particles at the beginning stages of clogging and that Z_C shows dependence upon the pore water velocity distribution of the unclogged gravel. Corroboration of the hypothesis can be explained due to the fact that Re^*, φ, and Re_K have been used as predictors of the pore water velocity and subsurface transport. A number of studies have used u_*, φ, and Re_K to predict the pore water velocity (Nagaoka and Ohgaki, 1990; Shimizu et al., 1990; Fries, 2007), and Nagaoka and Ohgaki (1990) use d_{ss}, which is correlated k_s, in their parameterization of pore water velocity. In the previously published pore water velocity equations, increases in Re^*, φ and Re_K result in the increased magnitude of the pore water velocity and extent of non-Darcian pore water deeper into the gravel substrate (Nagaoka and Ohgaki, 1990; Shimizu et al., 1990; Fries, 2007). Our significant dependence of Z_C^* upon Re^*, φ and Re_K in Figure 3 suggests a process where the fluid pore water velocity carries and disperses fine sediment particles deep into the gravel substrate. The dependence of Z_C^* upon Re^*, φ and Re_K for the deep clogged sediments support the hypothetical model by Gibson et al. (2011) that the

deepest multi-particle bridges likely occur temporarily early in the clogging process prior to arrival of the sediment front and filling of gravel pores near the water-sediment interface. For these conditions, the pore water velocity would be expected to reflect unclogged gravel conditions and thus show dependence on the Re^*, φ and Re_K parameters which do not account for the influence of the fines. The non-Darcian pore water velocity is initiated at the water-sediment interface due to upwhelling and downwelling, i.e., fluid pumping, at the stoss and lee side of large roughness grains (Reidenbach et al., 2010). The turbulent mechanism at the water-sediment interfaces diffuses in the downward vertical as fluid is transported through the pore spaces of gravels, interacts with gravel particles, and fluid energy is dissipated until the pore water velocity reaches the background Darcian velocity. Our results suggest that during this downward fluid process, fine sediments are transported downward vertically, disperse, decelerate, and then form multi-particle bridges.

Support of our hypothesis that Z_C is associated with the downward dispersion of fine particles in the beginning stages of clogging and is dependent upon the pore water velocity distribution of the unclogged gravel is also corroborated by the results of a number of related clogging and filtration studies, although the studies tend to have slightly different experimental setups and sediment conditions than those used in this study (Sakthivadivel and Einstein, 1970; Wu and Huang, 2000; Fries and Trowbridge, 2003; Dermisis and Papanicolaou, 2014). The pioneering laboratory column study by Sakthivadivel and Einstein (1970) observed the dependence of seepage fluid velocity in the substrate to vertically deepen the location of multi-particle bridges, suggesting an influence of pore water velocity on Z_C. The column studies by Wu and Huang (2000) also supported the influence of seepage fluid velocity upon clogging of fine sand in gravels with a larger quantity of fines depositing deeper into the gravel columns as the seepage velocity increased. The work of Fries and Trowbridge (2003) focused on the deposition of fines to the water-gravel interface and showed an enhancement of deposition as a function of Re^*. The Fries and Trowbridge (2003) result supports the pore water velocity hypothesis and that turbulent structure associated with large roughness elements has the potential to propel fine sediment into the gravel pore spaces.

Perhaps the most compelling result that agrees with our hypothesized dependence of Z_C upon pore water velocity is the recent paper Dermisis and Papanicolaou (2014), which focuses on the influence of boulders, i.e., isolated large roughness elements, in the streambed on sediment clogging. Dermisis and Papanicolaou (2014) show that the presence of boulders promote sediment intrusion of sand particles with the total amount of the infiltrated sand to be 44% greater when boulders were present. The presence of the boulders are expected to have increased the downwelling velocity at the water-sediment interface, thus increasing the pore water velocity distribution and transporting fines deeper into the streambed.

Somewhat surprisingly, the traditionally defined and adjusted bed-to-grain ratios ($\frac{d_{ss}}{d_{fs}\sigma_{ss}}$ and $\frac{d_{ss}}{d_{fs}}$) were weak predictors of Z_C^* for the experimental test results analyzed (see Table 2) despite the fact that the bed-to-grain ratio is the most widely discussed parameter in terms of the general clogging phenomena (Beschta and Jackson, 1979; Carling, 1984; Diplas and Parker, 1985; Wu and Huang, 2000; Fries and Trowbridge, 2003; Wooster et al., 2008; Cui et al., 2008; Gibson et al., 2008; Gibson et al., 2010; Gibson et al., 2011). The macro-analysis results suggest that the bed-to-grain ratio adds little to the prediction of Z_C^* for this class of noncohesive fine sediments and gravel-bed substrate so long as the experimental tests conditions are below the threshold for unimpeded static percolation ($Z_C<\infty$). The weak empirical dependence shown by $\frac{d_{ss}}{d_{fs}\sigma_{ss}}$ and $\frac{d_{ss}}{d_{fs}}$ upon Z_C^* can be partially attributed to the fact that d_{ss} can inversely control φ, with the latter being the single best direct predictor of Z_C^*. d_{ss} tends to be inversely proportional to φ as shown in Equation (10) as well as in the more general porosity equation for sands and gravel by Wu and Wang (2006) extended from the work of Komura (1963). We also emphasize that the tests for which $Z_C<\infty$ encompassed a fairly narrow range for d_{fs} from 80 to 630 μm. We do expect that d_{fs} plays a substantial role in the clogging processes due to its influence on multi-particle bridging (Valdes and Santamarina, 2008), however the empirical macro-analysis did not elucidate the role of the fines in this study. To this end, additional physics-based analysis of the bridging process is suggested in future research.

Empirical scaling of Z_C shows that φ and Re^* best collapse Z_C^* for the datasets tested in this analysis (see Figure 3d). The empirical result removed Re_K as a predictor, however φ is still represented in the result and accounts for the influence of gravel permeability. The collapse of the experimental tests resulting from the dimensional and statistical analyses of φ and Re^* offers promise in prediction of Z_C^*. By including the dispersion of the fine particles early in the clogging process, the dependence of the pore water velocity distribution can be accounted leading towards a better conceptual model of the clogging process. However, scatter remains in our data collapse shown in Figure 3. This scatter can in part be attributed to the estimation of porosity. Porosity can be particularly difficult to constrain given the non-monotonic behavior of porosity's dependence upon substrate particle size, shape, angularity, roughness, and wall effects. Streambed gravels are not perfectly spherical, smooth particles. Thus, we must rely on empirical porosity models to estimate this parameter when it was not directly measured. Although these empirical models tend to agree qualitatively, different simulation techniques and experimental methods may cause measurable differences. Another source of scatter can perhaps be attributed to the stochastic nature and measurement of clogging depth. Wooster et al. (2008), and Gibson et al. (2008, 2010, 2011) used a core sampling technique where cores were driven into the bed to remove a section of the clogged substrate. Even with careful precision, any movement of the substrate could cause further penetration of the fine sediment. For example, Beschta and Jackson (1979) tried using a core sampling technique but noted that inserting the core disturbed the gravels causing sand to move downwards and re-deposit. These problems associated with clogging depth measurement could be reflected in some of the scatter shown in Figure 3. Finally, further elucidating the explicit role of d_{fs} upon multi-particle bridging will be expected to further improve prediction of clogging. In the present study, d_{fs} did not prove to strongly influence the clogging depth, however, we caution the reader that our results should not be extrapolated to higher or lower values of d_{fs}, given that they are empirically based.

As a final point of discussion, we show how the empirical prediction of Z_C can be used to estimate the fine sand clogging profile within gravel bed substrate. The fine sand

clogging profile has been reported to decay exponentially from a maximum saturated fine sand fraction at the water-sediment interface to highly dispersed fines approach zero percent at depth in the streambed (Wooster et al., 2008; Dermisis and Papanicolaou, 2014). Based on these observations and results, we specify the fine sand fraction, f, in the clogging profile as

$$\frac{f}{f_s} = e^{-C_{exp}\, z}, \tag{17}$$

where f_s is the saturated fine sediment fraction and represents the maximum expected fine sediment fraction at the water-sediment interface and is a function of the gravel and sand porosity. C_{exp} is the coefficient for the exponential decay of the fine sediment fraction with depth in the profile and will be a function of Z_C. We estimate an f_s as

$$f_s = \varphi\left(1 - \varphi_{fs}\right), \tag{18}$$

where φ is the gravel porosity as specified in Table 1 and φ_{fs} is the porosity of the fine sand estimated using the porosity collapse of Wu and Wang (2006). We specify the coefficient for the exponential decay using the predicted clogging depth for the different experimental tests as

$$C_{exp} = \frac{ln\left(\frac{1\%}{f_s}\right)}{z_c}, \tag{19}$$

where we have approximated that the fine sand fraction decays to 1% at the predicted clogging depth. We provide comparison with the clogging profile estimated using the research of Wooster et al. (2008) where the profile was estimated as

$$\frac{f}{f_s} = \exp\left\{-0.0233\, \sigma_{ss}\left[\ln\left(\frac{d_{ss}\sigma_{ss}}{d_{fs}}\right) - 2.44\right]\left(\frac{z}{d_{ss}} - 2\right)\right\}, \tag{20}$$

where f_s was parameterized using theory and their experimental data as

$$f_s = \frac{0.62(1-0.621\sigma_{fs}^{-0.659})\sigma_{ss}^{-0.659}}{1-0.621^2(\sigma_{ss}\sigma_{fs})^{-0.659}} * \left[1 - \exp\left(-0.0146\frac{d_{ss}}{d_{fs}} + 0.0117\right)\right] \quad . \tag{21}$$

In Figure 6, we show parameterization of the clogging profile using Equations (17), (18) and (19) and the predicted clogging depth that includes the influence of pore water velocity on dispersion of particles to Z_C. The clogging profiles visually fit well with the measured experimental tests for which a clogging profile was reported, and visually tend to show an improved fit relative to the Wooster et al. (2008) Equations (20) and (21), especially for the Gibson et al. (2008, 2010 and 2011) datasets. The approach in Equations (17), (18) and (19) show an alternative approach to that of Wooster et al. (2008) with the former including the influence of pore water velocity on dispersion of particles to Z_C. The Wooster et al. (2008) approach has the advantage of being based solely on the substrate and fine sediment particle size distribution, however does not account for the dispersion processes early in clogging. The present approach in Equations (17), (18) and (19) empirically accounts for the pore water velocity influence however relies on additional parameters that must be estimated in analysis including the friction velocity and porosity.

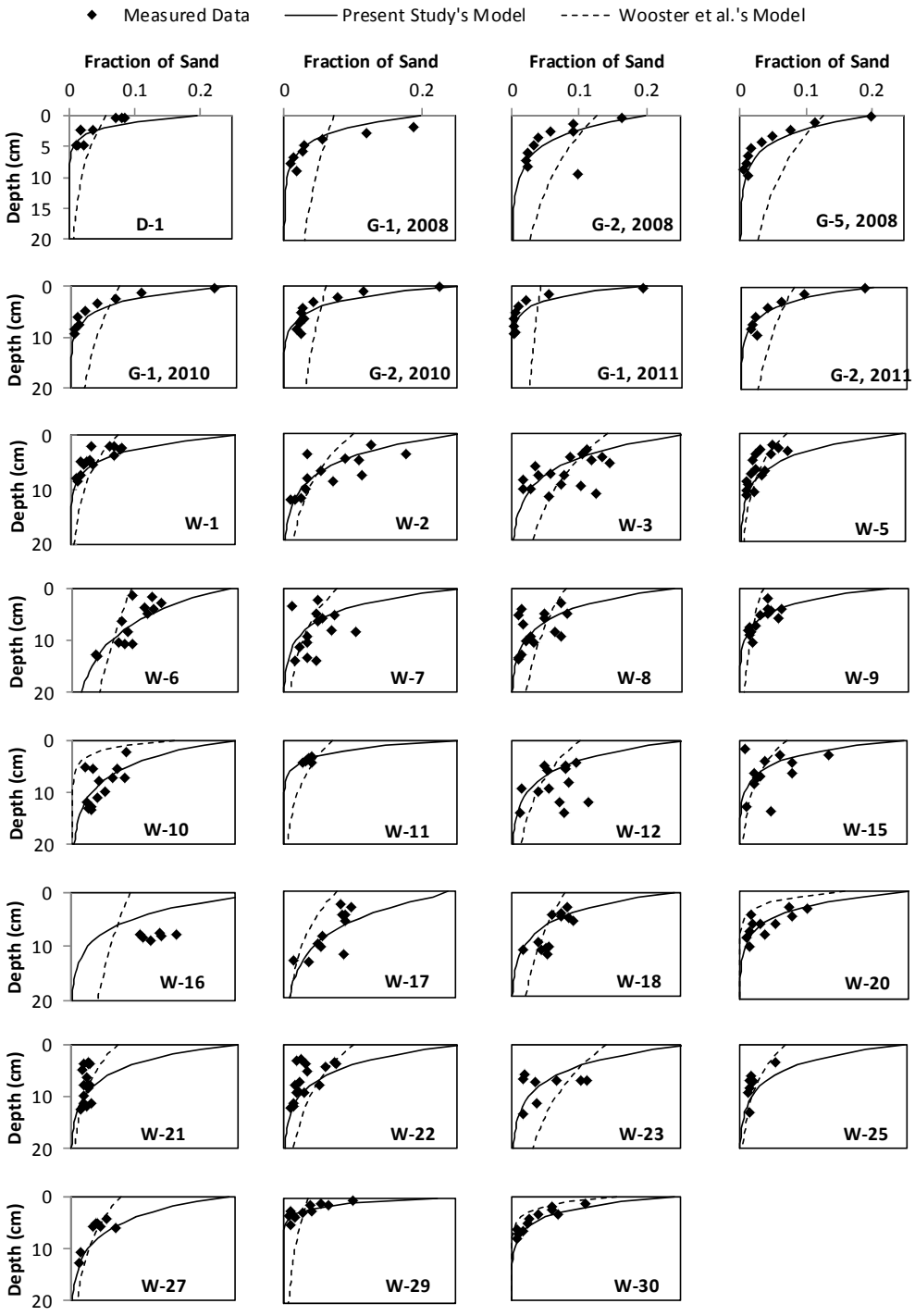

Figure 6. Exponential clogging profile using the approach in the present study as well as the approach in Wooster et al. (2008).

2.7 CONCLUSIONS

The meta-analysis results suggest that the adjusted bed-to-grain ratio is a reliable predictor of the initiation of clogging with clogging occurring below 27 for the fine fluvial sediment clogging in a gravel bed substrate for hydraulically rough turbulent flow in open channel flumes considered in this study. The original and adjusted bed-to-grain ratios show little influence on the depth of clogging once the lower threshold for bed filling is reached. Contrary to conventional wisdom, the bed-to-grain ratio is not used to predict the depth of clogging. Rather, results suggest that within this class of fines and gravel substrate sediments, the dimensionless clogging depth can be better collapsed using the substrate porosity and roughness Reynolds number reflecting the influence of pore water velocity upon fine sediment dispersion deep into the gravel pores. As a final step, the clogging depth results are used to estimate the clogging profile for fine sands in gravel substrate for the datasets.

A few comments are needed regarding use of the analysis and results presented here. First, the collapse of the dimensionless clogging depth is applicable to gravel substrate with fine sediment defined primarily as fine sand- and sand-sized particles. While one study included silt-sized grains, extension of the results to cohesive sediments resulting from particle size or organic matter content is cautioned. Cohesive sediment characteristics associated with chemical, biological and electromagnetic particle interaction could greatly impact the clogging of fines as could biofilm development within benthic substrate.

Second, all of the studies are performed in the laboratory and field verification of the dimensionless clogging depth is needed. We point out that datasets from field studies that measure clogging depth of fine sediment in gravel substrate have not been performed and future research of this topic is needed. With field studies in mind, we point out that the clogging depth is perhaps only one component of the clogging problem. Likely, streambed clogging is impacted by subsequent high water and sediment discharge events whereby the streambed clogged layers are mobilized and flushed. Thereafter, the

streambed could be re-clogged during subsequent low and moderate flow discharge events. These circumstances highlight the potential importance of low, moderate and high sediment transport events to the clogging problem and require further inclusion of the clogging processes into sediment transport modeling that considers mixed-grain sizes.

Finally, our results suggest that clogging depth prediction should shift from emphasis upon the bed-to-grain ratio to emphasis upon substrate porosity. To this end, we recognize that some scatter remains in the dimensionless clogging depth prediction *via* porosity (see Figure 3), and we suggest that further research should better constrain bed porosity in mixed-grain sediment transport studies. The main factors influencing porosity are grain size distribution and shape distribution, including shape, size, angularity, and roughness. There has been both theoretical and empirical porosity prediction models developed over the years. Unfortunately, due to the complexity introduced by particle shape variability, most of the research and developed models have been largely empirical. Although these empirical models tend to agree qualitatively, different experimental methods may cause quantitative differences. To this end, many researchers in other fields that focus on flow through porous media (e.g., industrial engineering) are using computer simulation to study and apply the properties of particle packing. There have been recent advances in 3D visualization, animation tools, and computational mechanics algorithms for porosity prediction (Latham et al., 2002). In order to better constrain streambed clogging for mixed-grain sediments, a more universally accurate, probability-based model of porosity might be developed and then verified with 3D computer simulations as well as traditional experimental measurements.

Chapter 3: Momentum-Impulse Model of Fine Sand Clogging Depth in Gravel Streambeds for Turbulent Open Channel Flow

3.1 SUMMARY

A momentum-impulse model that accounts for the critical impulse of a particle bridge that is balanced with a fluid pulse resulting from turbulent pumping is presented and applied for predicting the clogging depth of fine sand in gravel streambeds overlain by turbulent open channel flow. The model was tested against the literature-derived database of clogging depth with conditions defined by hydraulic flume experiments characterized by fine sand infiltrating into gravel substrates, with hydraulically rough open channel flow ranging from subcritical to critical conditions. Results show the efficacy of the momentum-impulse model application and support the hypothesis that particle bridging and intra-gravel flow due to fluid pumping control. Model results show improvement over previous empirical modeling of the clogging depth phenomena due to the reduction of unknown parameters from four coefficients to one coefficient and an increase in model predictability as quantified using k-fold validation and model comparison. A nomograph derived from running the momentum-impulse model is provided herein, which will be useful for stream restoration practitioners interested in estimating embeddedness. Also, we show prediction of the clogging profile using our clogging depth predicted with the momentum-impulse model, which is an additional application our work.

3.2 INTRODUCTION

Clogging of gravel streambeds is the process by which fine sands infiltrate and become lodged, i.e., clogged, within the pore spaces of gravel streambeds. The clogging of gravel bed rivers is characterized by an overlying hydraulically rough turbulent flow that acts to transport fine sediments and episodically pump them into the gravel interstices. Clogging of gravel bed rivers remains an important environmental process

for which prediction is currently needed due to its impacts on hyporheic exchange of nutrients for benthic ecosystem processes (Ford and Fox, 2014), fine clogged sediment can act as a sink for contaminants (Krou et al., 2006), and excessive infiltration of fine sediment into fish habitats, e.g., salmonid redds, can reduce oxygen supply to sustain life (Wood and Armitage, 1997).

Investigation of the clogging process has focused on experimental exploration and testing, typically in gravel-bed flumes in the hydraulics laboratory. Two early papers published in ASCE's *Journal of the Hydraulic Division* later renamed the *Journal of Hydraulic Engineering*, including Einstein (1968) and Sakthivadivel and Einstein (1970), were pivotal to providing a detailed description and conceptual model of the mechanisms controlling the clogging of gravel bed rivers. Einstein (1968) pioneered the first fine sediment infiltration into gravel beds experiments in a recirculating, laboratory flume in an effort to understand the mechanisms controlling excessive sediment infiltration. In his experiments, the channel bed was filled with gravel initially void of fine sediment, fine quartz was fed into the flume, and all of the fine sediment was observed to infiltrate to the bottom of the flume and proceeded to fill the gravel interstices upward. Sakthivadivel and Einstein (1970) investigated the spatial and temporal variation of fine sediment accumulation in a series of porous column experiments for a constant sediment input rate and flow through the column. Their results indicated that experiments with a smaller bed-to-grain ratio ($d_{ss}/d_{fs}=6.35$) fine sediment particles were deposited on top of the porous substrate, unable to infiltrate into the pores. When $7 < d_{ss}/d_{fs} < 15$, fine sediment completely infiltrated and clogged the porous medium over varying lengths of time. When the bed-to-grain ratio was greater than 15, fine sediment completely infiltrated through the porous column without being deposited within the porous substrate. Their results suggested that for $7 < d_{ss}/d_{fs} < 15$, a "bridging" mechanism was causing fine sediment particles to effectively clog the porous columns, while smaller fines passed through. Bridging occurs when multiple fine sediment particles collectively clog a pore space. Furthermore, Sakthivadivel and Einstein (1970) found that the probability of bridging to occur decreased linearly with an increasing vertical intra-gravel flow.

A series of clogging studies followed the early *Journal of the Hydraulic Division* papers. These later papers were published throughout the stream biology and water resources literature and heavily emphasized evaluations for the thresholds for clogging to occur as well as hydraulic and sediment factors impacting the clogging processes. Beschta and Jackson (1979) introduced the idea of the bed-to-grain ratio as being a controlling factor in the clogging process, which was further supported by a number of later papers (Carling, 1984; Diplas and Parker 1985; Wooster et al., 2008). Gibson et al. published a series of papers in (2008), (2010), and (2011) that focused on sand infiltration into gravel beds and observed that the bed-to-grain ratio greatly influenced the vertical trends of fine sediment in the gravel bed and suggested a threshold conditions for the bed-to-grain ratio that separates unimpeded static percolation from a definitive clogging depth. Chapter 1 of this thesis performed a meta-analysis of the existing studies and showed that an adjusted bed-to-grain ratio, $\frac{d_{ss}}{d_{fs}\sigma_{ss}}$, is a reliable predictor of the initiation of clogging for hydraulically rough turbulent flow in open channel flumes considered in the previous studies. After analyzing 146 experimental tests, we found a clear cutoff of $\frac{d_{ss}}{d_{fs}\sigma_{ss}}$ = 27 for the initiation of clogging (below 27) and unimpeded static percolation of fine sediments to the bottom of the experimental flumes (above 27). The result emphasized the dependence of porosity on clogging, particularly the dependence on the size of the pore space (Sakthivadivel and Einstein 1970; Valdes and Santamarina, 2006; Valdes and Santamarina, 2008).

While the threshold for clogging in gravel beds appears to be converging upon prediction with the adjusted bed-to-grain ratio, much ambiguity exists with regards to prediction of the clogging depth for conditions when the adjusted bed-to-grain ratio is less than 27. The process of fine sediment clogging in a gravel streambed is characterized by the deposition of fine particles to the top layer of the bed and intrusion of the fine particles onto the pore spaces of the gravel substrate (see Figure 1). Deposition of fines to the water-sediment interface occurs when the downward gravity and fluid pumping forces acting on the fine particles exceeds the force associated with upward turbulent ejections (Fries and Trowbridge, 2003). Upon transport below the water-

sediment interface, the fine particles can infiltrate to the sediment intrusion depth, decelerate, and then coalesce to form stable multi-particle bridges across pores in the gravel substrate (Sakthivadivel and Einstein, 1970). We refer to this relatively deep sediment intrusion depth with stable multi-particle bridges as the maximum clogging depth, Z_c (see Figure 2). Experimental observations of gravels clogged with fine sand has shown that the fraction of sand deposit is maximized near the water-sediment interface referred to as a "surface seal" and decreases exponentially to Z_c (Dermisis and Papanicolaou, 2014).

An early study by Beschta and Jackson (1979) suggested that Z_c showed a slight dependence on Froude number (Fr), however the later work of Carling (1984) found similar results over a range of Froude numbers, which tended to minimize the control of the bulk parameter upon Z_c. A number of studies have investigated the impact of the fine sediment input rate upon Z_c, and their results have minimized the influence of the fine sediment input rate upon Z_c (Diplas and Parker, 1985; Wooster et al., 2008). Huston and Fox (2014) investigated Z_c empirically using results of the previous studies and found that the dimensionless Z_c is best explained using the bed porosity (φ) and roughness Reynolds number (Re^*). Conceptually, the empirical results of Chapter 2 tend to agree well with the early description of clogging mechanisms highlighted in the early *Journal of the Hydraulic Division* papers by Einstein (1968) and Sakthivadivel and Einstein (1970) including the porosity's influence upon formulation of particle bridges within pore spaces of gravel beds and the porosity and Reynolds number's influence upon the intra-gravel velocity of the water to propel sand particles downward. However, there remains a lack of a physics-based prediction model of Z_c that simulates particle bridging and turbulent pumping to predict Z_c. The motivation of this chapter is formulation and testing of a physics-based model to predict Z_c for fine sand clogging of gravel substrate in turbulent open channel flow.

A particle bridge is a multi-particle structure characterized by the joining of two or more particles during the deposition process in a porous media in which each particle reaches a mutually stable configuration (Pugnaloni and Barker, 2004). Bridging may

occur following a number of different overlapping mechanisms: one being that an infiltrating sediment particle is retained in a pore by straining, effectively reducing the pore size, and another particle arriving at the pore combines with the previously retained particle to form a bridge across the pore throat; and secondly a fine sediment particle passing through a pore throat might be slightly retarded due to drag forces, and then a subsequent particle infiltrating behind it at a greater velocity may collide and form a bridge (Sakthivadivel and Einstein, 1970). In the case of particle bridging without the presence of water flow, bridge formation and stability are controlled by relative pore size-to-grain ratio, d_o/d_{fs}, bridge particle compression associated with skeletal forces, and particle shape (Sakthivadivel and Einstein, 1970; Valdes and Santamarina, 2006; Valdes and Santamarina, 2008). Fine sand clogging in gravels has been found to occur if d_o/d_{fs} is less than 5.5 when an overlying turbulent open channel flow is present. Valdes and Santamarina (2008) perform an experimental study and suggest that a ratio of d_o/d_{fs} less or equal to 4 to 5 will result in pore space clogging for spherical beads. The results from our meta-analysis as well as the fundamental work by Valdes and Santamarina (2008) emphasizes the concept that the clogging process is dependent upon the formation of particle bridges across substrate openings.

The particle bridging and hence clogging processes become more complex in the presence of a moving fluid (Sakthivadivel and Einstein (1970). In the case of turbulent open channel flow over a porous gravel bed, particle bridge formation and stabilization is expected to be impacted by the fluctuating velocity pulses associated with separation processes in the vicinity of particles within the turbulent boundary layer. Fluid pulses or pumping refers to the upwelling and downwelling at the stoss and lee side of grains due to its measure of the grain protrusion into the turbulent core of the flow. These protruding roughness elements along the streambed surface cause disruptions within the viscous sublayer to create pressure fluctuations near the sediment-water interface which result in fluid pumping (Li et al., 1994; Hutchinson & Webster, 1998; Reidenbach et al., 2010). This can form coherent eddies within the flow, which enhances the transport of fluid and suspended sediments to and from the sediment-water interface through the ejection of low momentum fluid from near the bed and the sweeping of high momentum

fluid toward the bed (Reidenbach et al., 2010). It has also been observed that flows over bed roughness have the potential to drive particles deeper with increasing roughness element size (Hutchinson and Webster, 1998; Fries and Taghon, 2010; Huettel and Rusch, 2000). Reidenbach et al. (2010) found that an increase in bed roughness substantially enhanced mass flux due to altering bed shear stresses. Furthermore, isolated large roughness elements have been reported to impact the fine sediment intrusion depth due to downwelling at the stoss (Dermisis and Papanicolaou, 2014).

Founded on the early principles published in in the early *Journal of the Hydraulic Division* papers by Einstein (1968) and Sakthivadivel and Einstein (1970), we hypothesized that the process of bridge formation and stability as well as fluid pumping during hyporheic exchange is closely related to and controls Z_c. We introduce a physics-based model that makes use of the momentum-impulse concept to estimate Z_c where the critical impulse of a particle bridge is balanced with a fluid pulse resulting from turbulent pumping. To this end, an increase in fluid pumping will result in an increased Z_c. The location of Z_c is established temporarily early in the sediment intrusion and clogging process prior to establishment of the exponential fine sediment profile associated with filling up and sealing of gravel pore spaces near the water-sediment interface (Gibson et al., 2011). It was also considered that an increase in fluid pumping may also cause the destabilization of particle bridges or decreases the probability of their formation. Based on the above conceptual model of particle bridging and turbulent pumping in turbulent open channel flow with fine sand and gravel bed, our objective was to formulate and test the physics-based model for estimating Z_c. The following steps were undertaken to meet our goal: (1) we formulate a physics-based model for *Zc* based the momentum-impulse processes impacting fine sediment bridge formation in a gravel substrate; (2) we test the model against the literature-derived database of Z_c and their corresponding sediment profiles described in Chapter 2; (3) we provide comparison of the physics-based model with a purely empirical model for Z_c and sediment profiles; (4) we provide a first nomograph that will be useful for estimating Z_c; and (5) we discuss advances in sediment transport needed to further develop the physics-based clogging model provided here.

3.3 MOMENTUM-IMPULSE MODEL FORMULATION

The momentum-impulse concept is used to combine the processes of particle bridging and turbulent bursting to impact the fine sand clogging in gravel beds overlain by turbulent open channel flow. The model is based on the concept that the momentum-impulse of a turbulent burst pulses down into the streambed, I_p. In order for clogging to occur, the turbulent pulse must be less than the bridging structure's critical impulse, I_{cr}, as

$$I_p < I_{cr} \quad . \tag{22}$$

In this manner, Equation (22) provides the threshold condition for particle bridging, and thus clogging, as impacted by a turbulent pulse into the streambed. To model the coupled process, I_{cr} and I_p are expressed using structural analysis of the bridge and fluid analysis of the turbulent pulse, respectively.

The critical impulse, I_{cr}, allowable by the bridged particles reflects the total potential energy of the structure at an unstable equilibrium point at which buckling can occur (Simitses and Hodges, 2005) and can be expressed as

$$I_{cr} = P_{cr} dt \quad , \tag{23}$$

where P_{cr} is the critical load upon the structure and dt is the time over which the momentum-impulse interacts with the structure. Failure and collapse of fine sized particles in bridges has been found to be initiated by a single particle that is located away from the centerline of the bridge structure (Valdes and Santamarina, 2008). Collapse occurs when a single particle rotates, becomes disconnected from its neighboring particles, and then slides in the downward vertical direction out of the bridge, which in turn causes the rest of the particles to collapse (see Figure 7a). The experimental findings of the failure mechanism of particle bridge collapse is consistent with the mechanics of compression-type arch bridge collapse (see Figure 7b). Arch bridges collapse by folding

up whereby an offset load produces cracking on the inner and outer curves of the arch's ring (Harvey, 2000). When the critical load is reached, the cracks act as hinges and the arch bridge is in a state of unstable equilibrium whereby the increase in the moment associated with the critical load causes rotation about the hinge at the bridge's base. Rotation is followed by sliding downward of the bridge sections at the crack where the critical load is located and thereafter folding up and collapse of the bridge occurs.

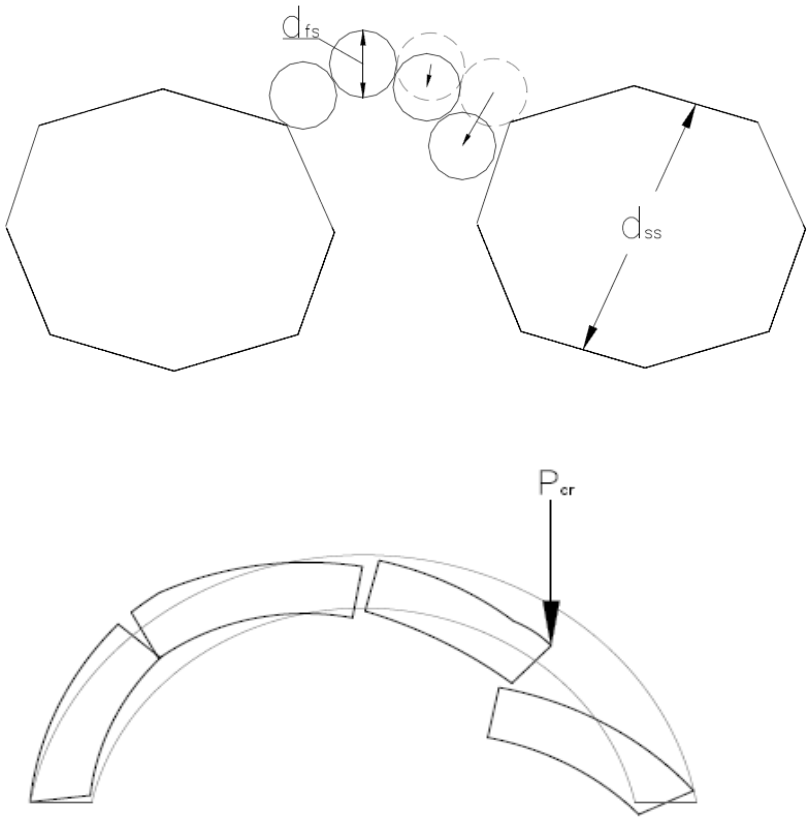

Figure 7. (a, top) Collapse of the particle bridge occurs when a single particle slides downward, out of the bridge. (b, bottom) Collapse of the particle bridge occurs when a critical load is reached which causes rotation about the hinge at the bridge's base.

Due to the similarities of the particle bridge and arch bridge processes, the particle bridge collapse can be expressed as occurring when a critical moment produced from the critical load rotates a single particle that then becomes dislodged and slides in the downward vertical direction. Using these failure mechanics, the critical load is estimated using the critical moment to cause rotation of the particle as

$$P_{cr} = \frac{1}{d_{cr}} M_{cr} \ , \tag{24}$$

where d_{cr} is the critical moment arm from the location of the offset critical load where particle rotation is initiated to the base of the bridge where the largest moment will occur (see Figure 8), and M_{cr} is the critical moment to rotate the particle. In order to express d_{cr} that is associated with bridge collapse, we consider a fairly stable class of bridges that minimize the interparticle angle between adjacent bridged particles and produce bridges that aligns along a semicircle that ends normal to the base of the structure (Valdes and Santamarina, 2008). Using the structure's geometry, d_{cr} can be calculated as a function of the diameter of the fine particles within the bridge, d_{fs}, and the number of particles in the bridge, n, as

$$d_{cr} = d_{fs}\left(\frac{1}{\tan\frac{90}{n}} - \frac{1}{2}\sin\frac{180}{n}\right). \tag{25}$$

From the bridge geometry in Figure 8, $d_{cr}{:}\,d_o$ is the ratio of d_{cr} relative to the bridge span, d_o, and will increase with n.

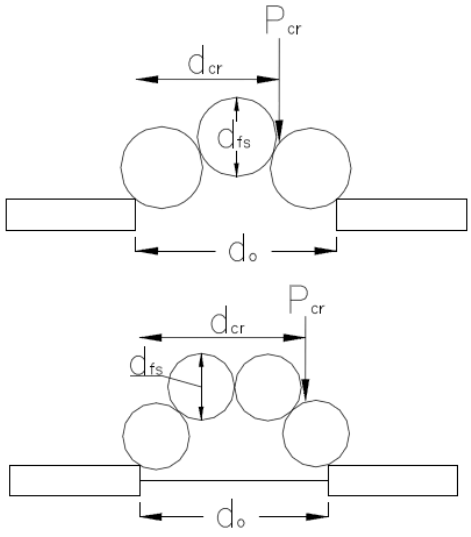

Figure 8. Geometric relationship between d_{cr}, d_o, and d_{fs}.

M_{cr} in Equation (24) is the critical moment that the particle-to-particle connection can withstand and considers the fact that the connections between adjacent particles must be able to absorb a structural moment for the bridge to be stable. The ability of the particle-to-particle connections to absorb a moment reflects the non-spherical nature of angular sand grains, which allow planar connectivity between particles, as opposed to pure moveable hinges. The moment that the particle connections can withstand will be proportional to the product of the moment arm from the edge of the face-to-face connection to the compression force between particles. We estimate the moment arm to be equal to the radius of the sand particle at the connection and the compression force to be equal to the half weight of the bridge structure given that rotation is initiated at the base of the bridge. In this manner, the critical moment associated with the structural connections is calculated as

$$M_{cr} = r_{fs} \frac{n}{2} W_p \ , \tag{26}$$

where r_{fs} is the radius of the sand particle at the connection and W_p is the particle weight expressed as

$$W_p = \rho_s g \frac{\pi}{6} d_{fs}^3 \tag{27}$$

where ρ_s is the particle density and g is gravitational acceleration.

In analysis of the structure's stability in Equation (23), the structure's potential ability to dampen, and thus its potential to withstand, the impulse force is also assessed through the critical impulse time, dt. Theoretically, the potential exists for the structure to withstand a theoretical ideal impulse force, i.e., impact, $\left(dt \to \frac{1}{\infty}\right)$ that excites all vibrational modes of the structure (Gambhir, 2004). More realistically, we cannot produce an ideal impulse force numerically, and we need to apply a load over a discrete amount of time. In this manner, dt is governed by the maximum mode frequency of the

structure that is expected to potentially cause disequilibrium, which can be expressed using the structure's maximum mode frequency (f_{max}) as

$$dt = \frac{1}{20 f_{max}} \ , \tag{28}$$

The f_{max} of the structure is dependent on the overall complexity of the structure, and in the case of bridged particles the vibrational mode frequency is parameterized by considering the number of free (non-fixed) hinges that may oscillate as

$$f_{max} = n - 1 \ . \tag{29}$$

The result in Equation (29) suggests that higher number particle structures have potential for higher modal vibration and thus a lower governing ideal impulse time step and lower potential critical impulse for the same load. For example, the critical impulse of a four particle bridge is 70% that of a three particle bridge for the same critical load.

The momentum-impulse of a turbulent associated burst will decay during fluid transport deeper into the bed. A turbulent burst in gravel beds produces a downwelling mass of fluid due to the sweeping of high momentum fluid to the streambed by coherent eddies in the flow (Reidenbach et al., 2010). Directly beneath the sediment-water interface the intra-gravel flow becomes non-Darcian due to periodic pressure fluctuations induced by coherent turbulent vortices near the streambed, e.g., turbulent pumping. These turbulent fluctuations induce a slip velocity at the sediment-water interface that has been found to decay exponentially with depth until it reaches Darcy velocity deep in the gravel bed. Experimental results, while limited, have measured velocity profiles and vertical mass transport in a porous medium beneath free surface flows (Shimizu et al., 1990). Shimizu et al. (1990) provided data and a model describing the exponential decay of vertical fluid velocity with depth after an initial velocity pulse at the sediment-water interface. Using the data of Shimizu et al. (1990), the velocity of the pulse has been parameterized using an exponential velocity decay of the slip velocity at the boundary with the exponential coefficient showing dependence upon the bed porosity, friction or slip velocity, frictional

characteristics of the fluid and substrate, and empirical calibration coefficients (Nagaoka and Ohgaki, 1990; Shimizu et al., 1990; Leonardson, 2010). We use a similar approach herein to estimate the velocity pulse at depth in the gravel substrate.

The net momentum-impulse associated with the turbulent burst that will interact with a particle bridge is formulated as

$$I_p = m_f u(z)_p \ , \tag{30}$$

where m_f is the mass of the fluid pulse and $u(z)_p$ is the velocity of the pulse, which is dependent upon the vertical depth (z) into the gravel substrate. The fluid mass of the pulse is expressed based on the projected size of the bridge that is impacted by the fluid pulse times the relative volume of the void through which the pulse is being transported as

$$m_f = \rho_f \varphi (n-1) \frac{\pi}{6} d_{fs}^3 \ , \tag{31}$$

where ρ_f is the density of the fluid, φ is the porosity, n is the number of particles in the bridge, and d_{fs} is the diameter of the fine sand particle. We approximate the velocity pulse at a depth in the gravel substrate as

$$u(z)_p = (u_s - u_d) exp\left(-c_p \frac{\nu \sigma_{ss}}{\varphi u_*} z\right) \ , \tag{32}$$

where u_s is the slip velocity at the substrate sediment-water interface that decays with depth into the substrate, ν is the kinematic viscosity of the fluid, σ_{ss} is the geometric deviation of the substrate sediment particle size distribution, u_* is the fluid friction velocity, and c_p is an empirical coefficient. u_s can be expressed using a relationship between slip velocity and interfacial diffusion (v_b) developed by Ruff and Gelhar (1972) as

$$(u_s - u_d)^3 + \frac{4}{3}\left(\frac{a}{b} + 2u_d\right)(u_s - u_d)^2 = 2\frac{u_*^4}{b\nu_b} \quad , \tag{33}$$

where

$$a = \frac{\nu}{K}, \tag{34}$$

$$b = \frac{1}{c\sqrt{K}} \quad , \tag{35}$$

and c is a coefficient set to 1.8 for sediment beds. Furthermore, Fries (2007) developed an empirical relationship between υ_b and the Peclet number (Re_k) as

$$\nu_b = \nu A_F Re_k^{B_F} \quad , \tag{36}$$

where

$$A_F = \begin{cases} 1.49 + \frac{0.52}{-0.39} & if\ 0.01 < Re_k < 1 \\ 1.65 + \frac{0.58}{-0.43} & if\ 1 < Re_k < 50 \end{cases} \quad \text{, and} \tag{37}$$

$$B_F = \begin{cases} 2.7 \pm 0.1 & if\ 0.01 < Re_k < 1 \\ 1.6 \pm 0.1 & if\ 1 < Re_k < 50 \end{cases} \quad . \tag{38}$$

The vertical component of Darcy's law is expressed as,

$$u_d = -K\frac{\partial h}{\partial z} \tag{39}$$

where K is the hydraulic conductivity of the gravel bed, and $\partial h/\partial z$ is the pressure head.

The model formulation in Equations (22) through (39) can be used to solve for the critical Z_c that provides the threshold condition for particle bridging in Equation (22). In this manner, we equate the momentum-impulse from the turbulent pulse and the critical

impulse of the particle bridge and solve for the unknown depth into the substrate, $z=Z_c$. Model application relies on hydraulic and sediment inputs including d_{fs}, d_{ss}, σ_{ss}, φ, K, u_*, v, Z_C, Re^* and Re_K. Model calibration and validation relies on adjusting a single unknown constant coefficient, namely c_p in Equation (32). c_p is unknown due to the lack of experimental data for decay of the velocity pulse within the gravel substrate. That is, Shimizu et al. (1990) and Nagaoka and Ohgaki (1990) investigated substrates that were larger in diameter and different in shape and smoothness than the gravel beds used in previously reported clogging studies.

3.4 MODEL TESTING

We applied the momentum-impulse model for available clogging data in literature obtained in the meta-analysis from Chapter 2 for clogging of fine fluvial sediment in a gravel bed substrate for hydraulically rough turbulent flow in open channel flumes. The meta-data was obtained from hydraulic flume experiments where hydraulic and sediment conditions can be controlled and Z_c measured. The experiments where characterized by fine sand depositing into clean porous gravel substrate and infiltrating until multi-particle bridging within the gravels or unimpeded static percolation occurred; hydraulically rough open channel flow ranging from subcritical to critical conditions, free of pronounced surface waves that could drive fine sand particles deeper into the bed; and free of mobilizing the gravel substrate which could result in the destabilization of multi-particle bridging causing further infiltration of fine sand particles into the gravel substrate. Of the 146 experimental tests investigated in Chapter 2 only 52 of these tests reported a clogging depth, i.e., the other 76 test were above the threshold condition for clogging. It is important to note that because Beschta and Jackon (1979) only reported a seal depth, their datasets of 18 experiments were not used in the model testing. Hydraulic and sediment conditions of the 52 tests are compiled in Table 1 including values for d_{fs}, d_{ss}, σ_{ss}, φ, K, u_*, v, Z_C, Re^* and Re_K.

The earliest research to report gavel bed clogging was performed by Beschta and Jackson (1970). They conducted flume tests with single size sand intruding a single gravel bed under varied water discharge, flume gradient, and fine sediment input rates. As previously discussed, Beschta and Jackson (1970), reported a seal depth and not Z_c (see seal depth in Figure 1). Diplas and Parker (DP) (1985) performed clogging experiments with two sizes of fine sand in a single gravel bed flume and varied the fine sediment input rate across a broad range. Wooster et al. (W) (2008) performed clogging experiments in a hydraulic flume across a wide range of gravel substrate conditions for a single sand size. Gibson et al. (G) published a series of papers in (2008), (2010), and (2011) that include ranges for sand size, gravel size and hydraulic conditions.

Fine sediment in all 52 studies compiled in Table 3 were fine sand to sand-sized grains. Gravel-beds ranged in size from approximately 2 to 17 mm. The majority of the studies were subcritical flow with some studies at or near critical conditions. All studies were hydraulically rough as indicated by Re^* greater than 100. Most of the parameters compiled in Table 3 were reported in the papers, however, some parameter were not directly reported and were approximated as described in Chapter 2.

The empirical coefficient C_p was optimized using the k-fold cross validation technique. The dataset, i.e. 52 tests in Table 3, was randomly divided into ten groups with seven tests in each group. Nine groups were used for training and one for testing. The training groups were plotted and fit with a linear regression line, which was optimized by adjusting the empirical coefficient C_p. The adjusted model was then ran to estimate Z_c for the testing data set and a root mean square error (RMSE) was calculated to ensure optimization, being minimum for the adjusted C_p.. This process was repeated nine times, until each group was used as both a training and a testing group, resulting in ten C_p values. An average C_p was calculated and used in the clogging model.

3.5 RESULTS AND DISCUSSION

Simulations of the modeled Z_c of fine sand in gravel-bed substrates *via* the momentum-impulse model were compared to the measured Z_c values collected by others

and compiled in the meta-analysis performed in Chapter 2 (see Figure 9). Due to the lack of experimental data for decay of the velocity pulse within the gravel substrate, a single empirical coefficient, C_p, was calibrated to a value of 18.8 using the k-fold validation technique. As a result of the cross validation, we found an $R^2 = 0.79$ when a linear regression line is fit to the modeled Z_c versus measured Z_c (see Figure 9). The result indicates that the momentum-impulse model reasonably predicts the clogging depth of fine sand in gravel substrates.

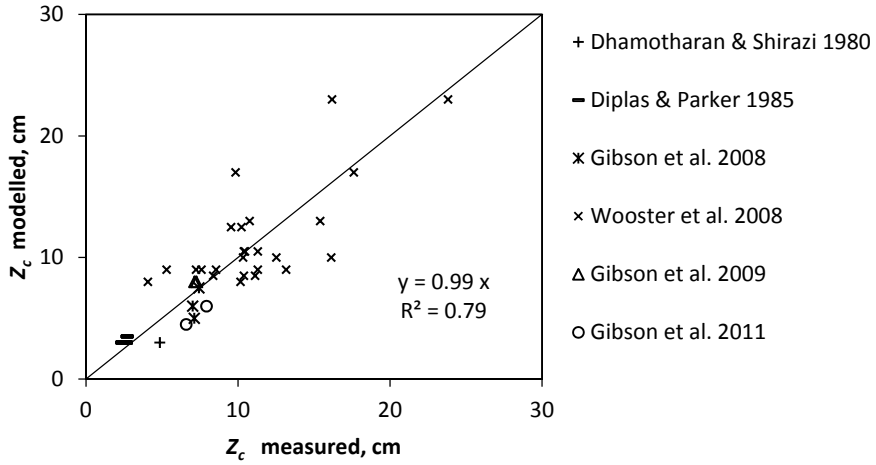

Figure 9. Momentum-Impulse Model vs. Measured Values of Z_c

The significance of $C_p = 18.8$ was investigated by comparing Equation (32) to measured subsurface velocity profiles provided by Shimizu et al. (1990). Shimizu et al. (1990) measured the vertical velocity profile of varying free surface flow conditions using a pitot tube inserted at various depths within the porous substrate. Equation (32), with $C_p = 18.8$, was used to calculate the vertical velocity profiles for the Shimizu et al. (1990) test conditions and then compared to the measured velocity profiles. This comparison indicates a similar exponential decay of subsurface velocity with depth, however, the measured slip velocities from Shimizu et al. (1990) were significantly larger than those predicted by Equation (32) for their experimental parameters. Hence, while the measured velocity profiles showed a similar exponential decay with depth, the velocities at the surface-water interface were larger than predicted by Equation (32). This discrepancy can be attributed to the fact that the substrate particles used by Shimizu et al.

(1990) were glass spheres with a diameter of 30 mm, which are larger than the gravel particles used to calibrate the momentum-impulse model. These larger particles may induce larger fluid pumping at the sediment-water interface, resulting in a larger slip velocity. Furthermore, it can be concluded that the momentum-impulse model may only be applicable for gravel substrates of sizes ranging from 2 – 17.5 mm.

The momentum-impulse model uses the combined processes of particle bridging and turbulent bursting to estimate Z_c of fine sand in a gravel bed overlain by turbulent open channel flow. This physical-based model is an improvement to the purely empirical Z_c model described in Chapter 2. While the empirical model was able to capture the essence of the two major processes that govern gravel bed clogging, i.e. particle bridging and turbulent bursting are represented by φ and Re*, the momentum impulse model is able to estimate clogging based on a more physically-based approach. In Figure 10, we compare the momentum-impulse model results to an empirical model derived from the scaling in Chapter 2. The coefficient of variance, R^2, revels a better linear regression fit for the momentum-impulse model results than the empirical model with an R^2 of 0.79 and 0.75 for the physical and empirical models, respectively. Hence, the momentum-impulse model shows an improvement with the amount of variance when fitted with a linear regression line. Similarly, both models show similar error due to bias. Model bias is the difference between simulated and measured values (Bullied et al., 2014) and when normalized by 10 cm, is calculated as follows,

$$Model\ Bias = \frac{1}{n}\sum_{i=1}^{n}(Z_c(model) - Z_c)/10\ cm. \tag{44}$$

The error due to model bias is 1% and 02% for the empirical model and momentum-impulse model, respectively. While the momentum-impulse model shows improvement to model accuracy when compared to the empirical model, it also decreases the number of empirical parameters from four to one, a notable improvement. The advancement is a major step towards the development of a purely theoretical model of the fine sand clogging of gravel bed streams overlain by turbulent open channel flow.

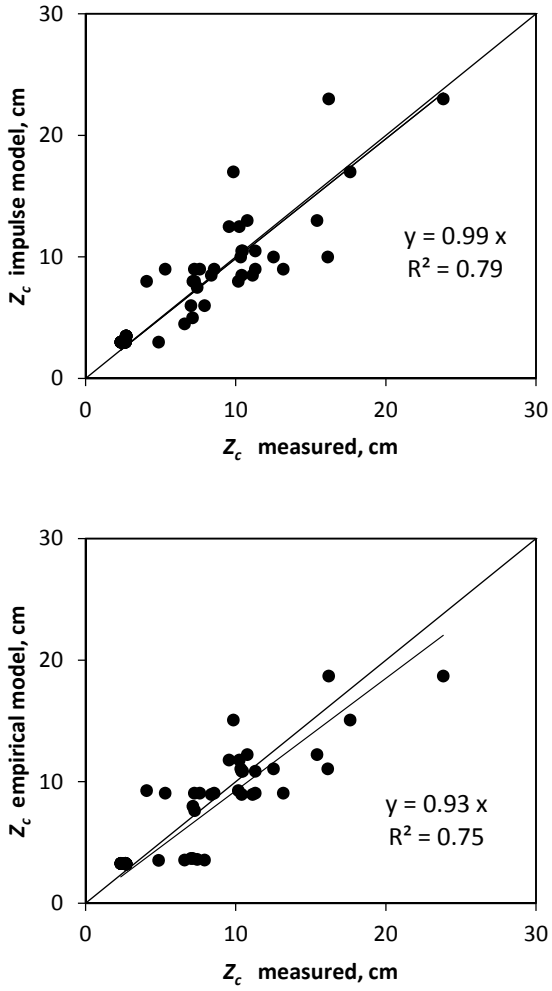

Figure 10. Shows comparison between the empirical model and the impulse model.

Although the modeled Z_c values show a linear trend with the observed values, some scatter remains. This discrepancy can in part be attributed to the estimation of d_o. The actual pore size of a gravel bed framework is difficult to constrain due to its dependence on substrate particle size, shape, angularity, roughness, and wall effects. Streambed gravels are not perfectly spherical, smooth particles. However, we must rely on geometrical relationships between perfect spheres to estimate the pore size, e.g. Heron's formula. Another source of scatter could be attributed to the actual measurement of the clogging depth. Due to the non-cohesive nature of fine sands and gravitational forces always pulling the fine sand downward, any disturbance to the substrate could cause further penetration of the fine sediment. For example, Wooster et al. (2008), and

Gibson et al. (2008, 2011) used a core sampling technique where cores were driven into the bed to remove a section of the clogged substrate. This process could easily dislodge fine sediment particles destabilizing the particle bridges, and result in further infiltration. To this end, Beschta and Jackson (1979) reported that core sampling disturbed the gravel substrate causing sand to infiltrate further and re-deposit. These problems associated with clogging depth measurement could be reflected in the discrepancy between the model's results and observed values.

With the development of a physics-based model for *Zc* based on the momentum-impulse processes impacting fine sediment bridge formation in a gravel substrate, we used the validated model to show the behavior and prediction of Z_c under a range of hydraulic and sediment conditions that are well within the ranges investigated in this paper. The various sediment and hydraulic conditions investigated include d_{ss}, φ, u_*, and σ_{ss}. d_{ss} was applied over the range 2 mm to 17 mm, by 1 mm increments. The remaining variables were varied to coincide with the median ± one standard deviation of the meta-data used to calibrate the momentum-impulse model. A nomograph was developed by modeling 432 different combinations of d_{ss}, φ, u_*, and σ_{ss}. (see Figure 11). As can be seen from the nomograph, Z_c increases with φ and u_*, and decreases with σ_{ss}. The dashed vertical line represents the threshold for unimpeded static percolation shown in Figure 2. It is important to note that these nomographs were developed using a single d_{fs} equal to 0.35 mm, the average fine sediment size of the meta-data.

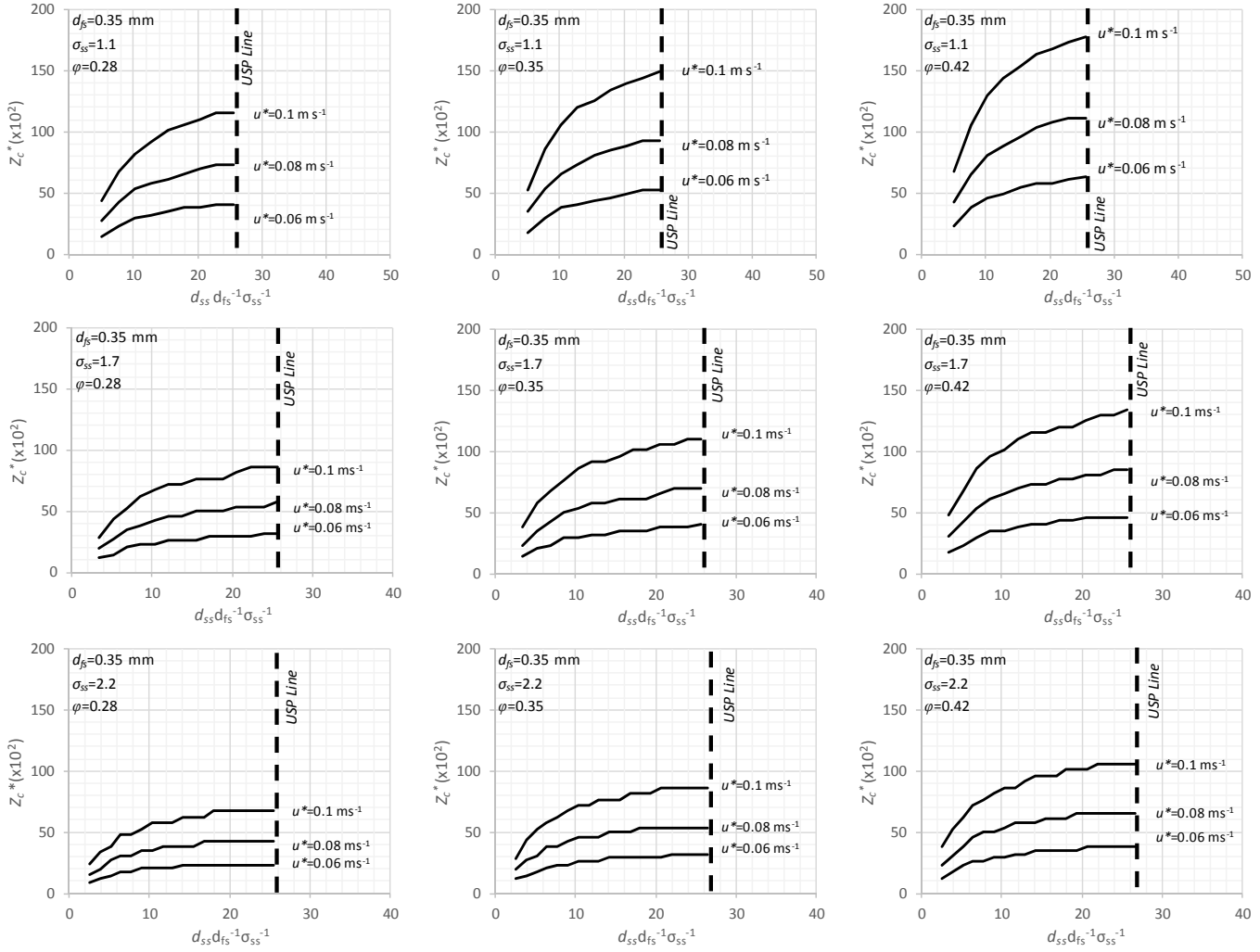

Figure 11. Nomographs developed from the impulse model.

It is believed that excessive fine sediment is the leading cause of impairment for streams and rivers in the United States, the Z_c nomograph provide a first estimate for stream restoration scientists and engineers. Excessive fine sediment can have a number of negative impacts on gravel bed stream and river systems. In particular, these excessive fine sediments can degrade salmon spawning habitats through the clogging of salmonoid redds. As fine sediment infiltrates and forms a clogging layer in a gravel bed deposit dissolved oxygen and hyporheic exchange of nutrients subsequently decreases, and effectively smothers salmon eggs (Suttle et al. 2004). Gravel beds also serve as shelter, feeding habitat, and spawning habitat for macroinvertibrates. Excessive fine sediments decrease the availability of pore spaces within the substrate, decreasing suitable habitat for macroinvertibrates. An increase in clogged fine sediment decreases the amount of nutrients deposited and retained in the substrate, limiting macroinvertibrates food supply (Bo et al., 2007). To this end, the Z_c nomograph can be incorporated into sediment transport models used in future stream restoration projects to estimate the environmental impact of fine sediment pulses into gravel bed systems due to land-use changes such as nearby construction or dam removal. Understanding the stream system's response to fine sediment loads, especially the depth to which fine sediment will clog in gravel beds, will help stream restoration scientists and engineers estimate the stream's embeddedness, which is measure of the degree to which substrate gravels are buried in fine sediment (Rosgen, 1996). A stream's embeddedness is one of the criteria used to biologically assess a stream's quality. Hence, knowing the clogging depth associated with certain hydraulic and sediment conditions can allow stream restoration scientists and engineers to quickly estimate a stream's embeddedness in response to potential increases in fine sediment loads.

Similar to Chapter 2, we show how the momentum-impulse modeled Z_c can be used to estimate the fine sand clogging profile within gravel bed substrate. The fine sand clogging profile has been reported to decay exponentially from a maximum saturated fine sediment fraction at the sediment-water interface to highly dispersed fines approach zero percent at depth in the streambed (Wooster at al., 2008; Gibson et al., 2008; Gibson et al., 2010; Gibson et al., 2011; Dermisis and Papanicolaou, 2014). Based on these

observations and results, we specify the fine sediment fraction, f, in the clogging profile as

$$\frac{f}{f_s} = e^{-C_{exp}z}, \quad (45)$$

where f_s is the saturated fine sediment fraction and represents the maximum expected fine sediment fraction at the sediment-water interface and is a function of the gravel and sand porosity. C_{exp} is the coefficient for the exponential decay of the fine sediment fraction with depth in the profile and will be a function of Z_c. We estimate an f_s as

$$f_s = \varphi(1 - \varphi_{fs}), \quad (46)$$

where φ is the gravel porosity as specified in Table 3 and φ_{fs} is the porosity of the fine sand estimated using porosity collapse of Wu and Wang (2006). We specify the coefficient for the exponential decay using the predicted clogging depth for the different tests as

$$C_{exp} = \frac{\ln(\frac{3\%}{f_s})}{Z_c}, \quad (47)$$

where we have approximated that the fine sand fraction decays to 3% at the predicted clogging depth. The fine sediment fraction at Z_c was optimized for the momentum-impulse model by minimizing the Sum Square Error.

In Figure 12, we show parameterization of the clogging profile using Equations (45), (46) and (47) and the momentum-impulse model predicted Z_c along with the clogging profiles from Chapter 2. The clogging profiles visually fit well with the meta-data collected in Chapter 2 and show a similar predicted fine sediment profile from the empirical clogging model developed in Chapter 2.

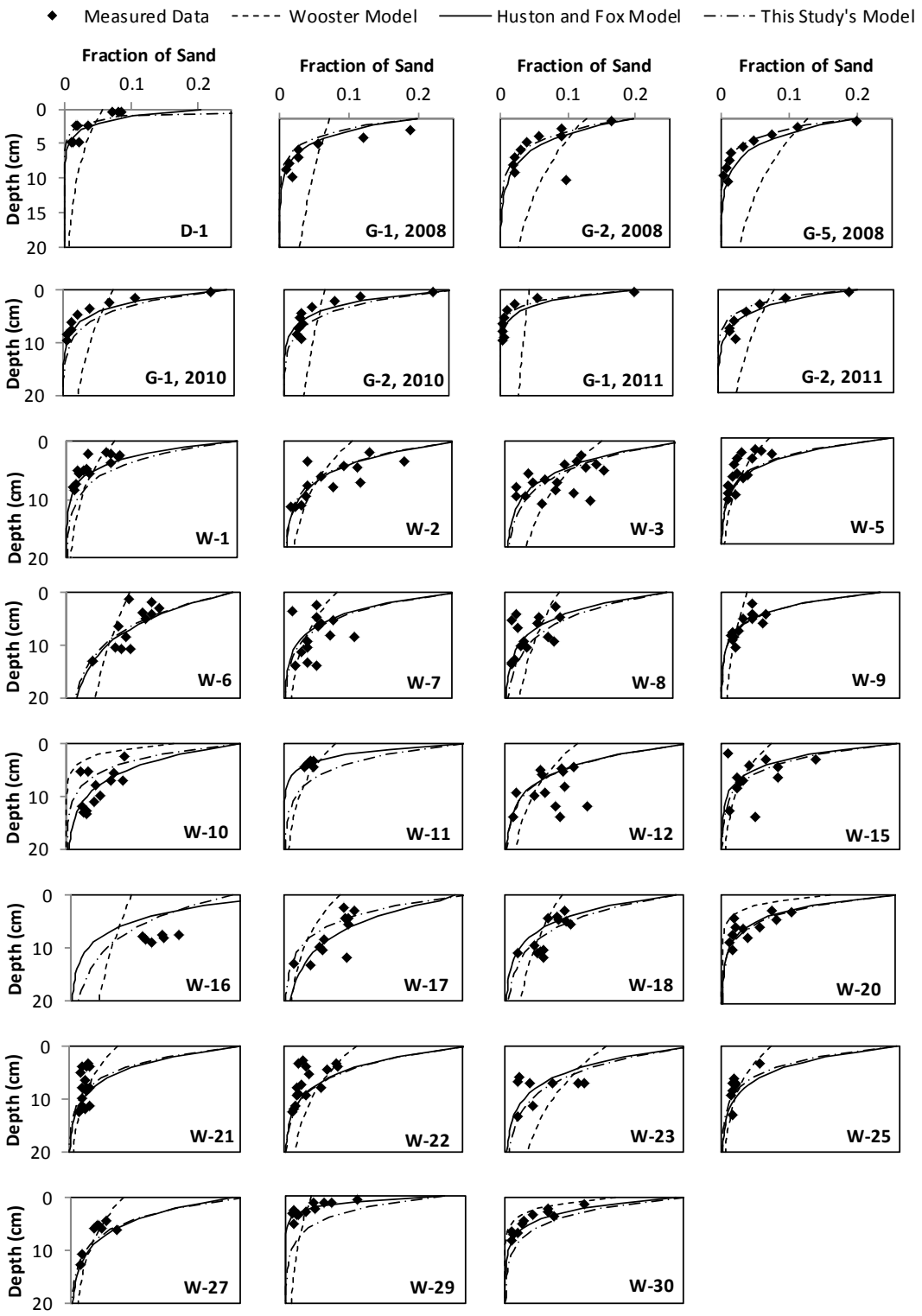

Figure 12. Exponential clogging profile using the approach in the present study as well as the approach in Wooster et al. (2008) and Chapter 2.

3.6 CONCLUSIONS

The work here shows that the newly formulated momentum-impulse model can be appropriately used to provide a physics-based model for sand clogging in gravel substrate overlain by turbulent open channel flow. The results support the hypothesis that particle bridging and intra-gravel flow associated with turbulent fluid pumping control the clogging depth (Z_c). With the development of the momentum-impulse model, we have improved upon the understanding of the physical processes that govern the clogging depth of fine sand in gravel bed streams as well as provided a predictive tool that advances over previous modeling. The nomograph provided here provides an easy to use tool for restoration engineers. Restoration scientists and engineers can further use this information when designing constructed riffles. It is important to optimize bed porosity to allow for hyporheic exchange but limiting clogging depth. Furthermore, optimizing the channel design to decrease bed shear stress and fluid pumping can be achieved by adjusting the channel's width to depth ratio and bed roughness height.

We successfully modeled the process of turbulent bursting at the sediment water interface sending pulses of sediment-laden fluid into the streambed which carry fine sands to a certain depth at which particle bridging, and subsequently clogging, occurs. However, there remains the lack of a purely theoretical prediction of the clogging depth because we use the empirical coefficient, C_p, to parameterize the vertical decay of the velocity pulse within the gravel bed over a wide range of conditions. To reduce this empiricism, new experimental data and fundamental modeling are needed to better understand turbulent-induced pulses into gravel streambed. As more information becomes available, we expect that the physical based approach presented here can be built upon. Finally, we are lacking field data for verification. While the momentum-impulse model can be used by restoration engineers as an initial estimate of clogging depth, field verification is needed. Various field data collection techniques such as frozen core sampling (Lisle, 1989) and burying sediment traps into the porous substrate (Frostick et al., 1984) can be used in future research to further calibrate and validate the momentum-impulse model reported here. Furthermore, it is recognized that the substrate

size range investigated in this thesis, i.e. 2 mm -22 mm, is smaller than most constructed riffles designed by restoration engineers, and further research is needed for larger substrate sizes.

APPENDICES

Table 2. Macro-analysis of clogging studies. Notes: (γ) E is Einstein (1968); DS is Dhamotharan and Shirazi (1980); BJ is Beschta and Jackson (1979); C is Carling (1984); DP is Diplas and Parker (1985); W is Wooster et al. (2008); G08, G10 and G11 are Gibson et al. (2008), (2010) and (2011); K is Kuhnle et al. (2013). (w) denotes porosity values calculated using empirical porosity equation from Wooster et al. (2008), while all other porosity values were provided by the authors. (ε) ∞ denotes unimpeded static percolation. ^{s} denotes the seal depth.

Test$^{\gamma}$	d_{fs} (mm)	d_{ss} (mm)	σ_{ss}	k_s (mm)	u^* (ms^{-1})	φ	K (ms^{-1})	ν (ms^{-2})	Fr	Re^*	Re_K	Z_c $(cm)^{\varepsilon}$
E-1	0.02	22.2	2.29	37.3	0.04	0.36	$3.14x10^{-7}$	$1.00\ x10^{-6}$	0.46	1559	23.3	∞
E-2	0.02	22.2	2.29	37.3	0.04	0.36	$3.14\ x10^{-7}$	$1.00\ x10^{-6}$	0.23	1559	23.3	∞
E-3	0.02	22.2	2.29	37.3	0.04	0.36	$3.14\ x10^{-7}$	$1.00\ x10^{-6}$	0.23	1559	23.3	∞
E-4	0.02	22.2	2.29	37.3	0.04	0.36	$3.14\ x10^{-7}$	$1.00\ x10^{-6}$	0.23	1559	23.3	∞
E-5	0.02	22.2	2.29	37.3	0.07	0.36	$3.14\ x10^{-7}$	$1.00\ x10^{-6}$	0.13	2701	40.3	∞
E-6	0.02	88.9	2.29	149	0.07	0.36	$5.02\ x10^{-6}$	$1.00\ x10^{-6}$	0.14	10002	149.4	∞
E-7	0.02	88.9	2.29	149	0.05	0.36	$5.02\ x10^{-6}$	$1.00\ x10^{-6}$	0.2	7073	105.7	∞
E-8	0.02	88.9	2.29	149	0.05	0.36	$5.02\ x10^{-6}$	$1.00\ x10^{-6}$	0.41	7073	105.7	∞
E-9	0.02	22.2	2.29	37.3	0.04	0.36	$3.14\ x10^{-7}$	$1.00\ x10^{-6}$	0.23	1559	23.3	∞
E-10	0.02	22.2	2.29	37.3	0.04	0.36	$3.14\ x10^{-7}$	$1.00\ x10^{-6}$	0.23	1559	23.3	∞
E-11	0.02	22.2	2.29	37.3	0.04	0.36	$3.14\ x10^{-7}$	$1.00\ x10^{-6}$	0.46	1559	23.3	∞
BJ-1	0.5	15	1.58	20	0.07	0.35	$1.28\ x10^{-7}$	$1.52\ x10^{-6}$	0.82	982	17.5	3^{s}
BJ-2	0.5	15	1.58	20	0.09	0.35	$1.28\ x10^{-7}$	$1.52\ x10^{-6}$	1.07	1243	22.2	6^{s}
BJ-3	0.5	15	1.58	20	0.11	0.35	$1.28\ x10^{-7}$	$1.52\ x10^{-6}$	1.24	1421	25.4	9^{s}
BJ-4	0.5	15	1.58	20	0.08	0.35	$1.28\ x10^{-7}$	$1.52\ x10^{-6}$	0.91	1087	19.4	3^{s}
BJ-5	0.5	15	1.58	20	0.1	0.35	$1.28\ x10^{-7}$	$1.52\ x10^{-6}$	1.26	1363	24.4	6^{s}
BJ-6	0.5	15	1.58	20	0.11	0.35	$1.28\ x10^{-7}$	$1.52\ x10^{-6}$	1.05	1391	24.9	9^{s}
BJ-7	0.5	15	1.58	20	0.08	0.35	$1.28\ x10^{-7}$	$1.52\ x10^{-6}$	0.87	1070	19.1	3^{s}
BJ-8	0.5	15	1.58	20	0.11	0.35	$1.28\ x10^{-7}$	$1.52\ x10^{-6}$	1.18	1422	25.4	6^{s}
BJ-9	0.5	15	1.58	20	0.1	0.35	$1.28\ x10^{-7}$	$1.52\ x10^{-6}$	1.02	1337	23.9	9^{s}

Table 2 (continued)

Test[γ]	d_{fs} (mm)	d_{ss} (mm)	σ_{ss}	k_s (mm)	u^* (ms^{-1})	φ	K (ms^{-1})	ν (ms^{-2})	Fr	Re^*	Re_K	Z_c $(cm)^{\varepsilon}$
BJ-10	0.5	15	1.58	20	0.08	0.35	1.28×10^{-7}	1.52×10^{-6}	0.83	1023	18.3	3^{s}
BJ-11	0.5	15	1.58	20	0.1	0.35	1.28×10^{-7}	1.52×10^{-6}	1.13	1375	24.6	6^{s}
BJ-12	0.5	15	1.58	20	0.1	0.35	1.28×10^{-7}	1.52×10^{-6}	0.97	1301	23.3	9^{s}
BJ-13	0.5	15	1.58	20	0.08	0.35	1.28×10^{-7}	1.52×10^{-6}	0.82	1060	19	3^{s}
BJ-14	0.5	15	1.58	20	0.1	0.35	1.28×10^{-7}	1.52×10^{-6}	1.05	1342	24	6^{s}
BJ-15	0.5	15	1.58	20	0.11	0.35	1.28×10^{-7}	1.52×10^{-6}	1.07	1422	25.4	9^{s}
BJ-16	0.5	15	1.58	20	0.08	0.35	1.28×10^{-7}	1.52×10^{-6}	0.85	1111	19.9	3^{s}
BJ-17	0.5	15	1.58	20	0.1	0.35	1.28×10^{-7}	1.52×10^{-6}	1.03	1301	23.3	6^{s}
BJ-18	0.5	15	1.58	20	0.11	0.35	1.28×10^{-7}	1.52×10^{-6}	1.05	1409	25.2	9^{s}
BJ-19	0.2	15	1.58	20	0.08	0.35	1.28×10^{-7}	1.52×10^{-6}	0.63	1057	18.9	∞
BJ-20	0.2	15	1.58	20	0.1	0.35	1.28×10^{-7}	1.52×10^{-6}	1.12	1353	24.2	∞
DS-1	0.12	2.25	2.75	5.62	0.05	0.34	2.68×10^{-9}	1.00×10^{-6}	-	280	2.6	4.86
C-1	0.19	16	2.12	50	0.12	0.39	2.29×10^{-7}	1.00×10^{-6}	0.76	5750	55	∞
C-2	0.19	16	2.12	50	0.06	0.39	2.29×10^{-7}	1.00×10^{-6}	0.1	2850	27.2	∞
C-3	0.19	16	2.12	50	0.02	0.39	2.29×10^{-7}	1.00×10^{-6}	0.01	900	8.6	∞
C-4	0.19	16	2.12	50	0.12	0.39	2.29×10^{-7}	1.00×10^{-6}	0.22	5750	55	∞
C-5	0.19	16	2.12	50	0.09	0.39	2.29×10^{-7}	1.00×10^{-6}	0.66	4300	41.1	∞
C-6	0.19	16	2.12	50	0.11	0.39	2.29×10^{-7}	1.00×10^{-6}	0.71	5400	51.6	∞
C-7	0.15	16	2.12	50	0.21	0.39	2.29×10^{-7}	1.00×10^{-6}	1.22	10600	101.3	∞
C-8	0.15	16	2.12	50	0.15	0.39	2.29×10^{-7}	1.00×10^{-6}	0.83	7450	71.2	∞
C-9	0.15	16	2.12	50	0.12	0.39	2.29×10^{-7}	1.00×10^{-6}	0.88	6150	58.8	∞
C-10	0.15	16	2.12	50	0.09	0.39	2.29×10^{-7}	1.00×10^{-6}	0.32	4350	41.6	∞
C-11	0.15	16	2.12	50	0.06	0.39	2.29×10^{-7}	1.00×10^{-6}	0.09	2900	27.7	∞
C-12	0.15	16	2.12	50	0.09	0.39	2.29×10^{-7}	1.00×10^{-6}	0.37	4500	43	∞
C-13	0.15	16	2.12	50	0.14	0.39	2.29×10^{-7}	1.00×10^{-6}	0.62	6800	65	∞
C-14	0.15	16	2.12	50	0.09	0.39	2.29×10^{-7}	1.00×10^{-6}	0.11	4250	40.6	∞
C-15	0.15	16	2.12	50	0.09	0.39	2.29×10^{-7}	1.00×10^{-6}	0.88	4500	43	∞
C-16	0.15	16	2.12	50	0.08	0.39	2.29×10^{-7}	1.00×10^{-6}	0.54	3900	37.3	∞

Table 2 (continued)

Test[γ]	d_{fs} (mm)	d_{ss} (mm)	σ_{ss}	k_s (mm)	u^* (ms^{-1})	φ	K (ms^{-1})	ν (ms^{-2})	Fr	Re^*	Re_K	Z_c $(cm)^{\varepsilon}$
C-17	0.15	16	2.12	50	0.1	0.39	2.29×10^{-7}	1.00×10^{-6}	0.53	4900	46.8	∞
C-18	0.15	16	2.12	50	0.11	0.39	2.29×10^{-7}	1.00×10^{-6}	0.8	5600	53.5	∞
C-19	0.15	16	2.12	50	0.13	0.39	2.29×10^{-7}	1.00×10^{-6}	1.11	6300	60.2	∞
C-20	0.15	16	2.12	50	0.12	0.39	2.29×10^{-7}	1.00×10^{-6}	1.1	6150	58.8	∞
C-21	0.15	16	2.12	50	0.16	0.39	2.29×10^{-7}	1.00×10^{-6}	0.95	7850	75.1	∞
C-22	0.15	16	2.12	50	0.16	0.39	2.29×10^{-7}	1.00×10^{-6}	0.95	7850	75.1	∞
DP-1	0.11	2.44	2.75	6	0.059	0.34	3.15×10^{-9}	1.00×10^{-6}	-	356	3.3	2.7
DP-2	0.11	2.44	2.75	6	0.057	0.34	3.15×10^{-9}	1.00×10^{-6}	-	342	3.2	2.7
DP-3	0.11	2.44	2.75	6	0.057	0.34	3.15×10^{-9}	1.00×10^{-6}	-	344	3.2	2.7
DP-4	0.11	2.44	2.75	6	0.057	0.34	3.15×10^{-9}	1.00×10^{-6}	-	344	3.2	2.7
DP-5	0.11	2.44	2.75	6	0.057	0.34	3.15×10^{-9}	1.00×10^{-6}	-	343	3.2	2.7
DP-6	0.11	2.44	2.75	6	0.057	0.34	3.15×10^{-9}	1.00×10^{-6}	-	343	3.2	2.7
DP-7	0.11	2.44	2.75	6	0.045	0.34	3.15×10^{-9}	1.00×10^{-6}	-	272	2.5	2.35
DP-8	0.11	2.44	2.75	6	0.046	0.34	3.15×10^{-9}	1.00×10^{-6}	-	274	2.6	2.35
DP-9	0.11	2.44	2.75	6	0.046	0.34	3.15×10^{-9}	1.00×10^{-6}	-	275	2.6	2.35
DP-10	0.11	2.44	2.75	6	0.046	0.34	3.15×10^{-9}	1.00×10^{-6}	-	277	2.6	2.35
DP-11	0.11	2.44	2.75	6	0.046	0.34	3.15×10^{-9}	1.00×10^{-6}	-	276	2.6	2.35
DP-12	0.11	2.44	2.75	6	0.046	0.34	3.15×10^{-9}	1.00×10^{-6}	-	276	2.6	2.35
DP-13	0.08	2.44	2.75	6	0.047	0.34	3.15×10^{-9}	1.00×10^{-6}	-	280	2.6	2.65
DP-14	0.08	2.44	2.75	6	0.047	0.34	3.15×10^{-9}	1.00×10^{-6}	-	280	2.6	2.65
DP-15	0.08	2.44	2.75	6	0.047	0.34	3.15×10^{-9}	1.00×10^{-6}	-	280	2.6	2.65
DP-16	0.08	2.44	2.75	6	0.047	0.34	3.15×10^{-9}	1.00×10^{-6}	-	280	2.6	2.65
DP-17	0.08	2.44	2.75	6	0.047	0.34	3.15×10^{-9}	1.00×10^{-6}	-	281	2.6	2.65
DP-18	0.08	2.44	2.75	6	0.047	0.34	3.15×10^{-9}	1.00×10^{-6}	-	281	2.6	2.65
DP-19	0.08	2.44	2.75	6	0.047	0.34	3.15×10^{-9}	1.00×10^{-6}	-	281	2.6	2.65
W-1	0.35	8	1.82	13	0.08	0.42[w]	7.77×10^{-8}	1.00×10^{-6}	0.51	1000	21.4	7.6
W-2	0.35	11.2	1.74	19	0.08	0.43[w]	1.74×10^{-7}	1.00×10^{-6}	0.51	1461	32.1	11.3
W-3	0.35	16	1.67	20.5	0.08	0.44[w]	4.01×10^{-7}	1.00×10^{-6}	0.51	1576	48.7	10.2

Table 2 (continued)

Test[γ]	d_{fs} (mm)	d_{ss} (mm)	σ_{ss}	k_s (mm)	u^* (ms^{-1})	φ	K (ms^{-1})	ν (ms^{-2})	Fr	Re^*	Re_K	Z_c (cm)[ε]
W-4	0.35	17.5	1.17	21	0.08	0.56 [w]	1.56×10^{-6}	1.00×10^{-6}	0.51	1615	95.9	∞
W-5	0.35	8	1.9	16	0.08	0.41 [w]	6.86×10^{-8}	1.00×10^{-6}	0.51	1230	20.1	10.4
W-6	0.35	8	1.23	10	0.08	0.54 [w]	2.72×10^{-7}	1.00×10^{-6}	0.51	769	40.1	17.6
W-7	0.35	8.5	1.72	19	0.08	0.43 [w]	1.04×10^{-7}	1.00×10^{-6}	0.51	1461	24.8	10.3
W-8	0.35	8	1.46	11	0.08	0.48 [w]	1.53×10^{-7}	1.00×10^{-6}	0.51	846	30	10.8
W-9	0.35	4	1.65	8	0.08	0.45 [w]	2.60×10^{-8}	1.00×10^{-6}	0.51	615	12.4	10.2
W-10	0.35	8	1.82	13	0.08	0.42 [w]	7.77×10^{-8}	1.00×10^{-6}	0.51	1000	21.4	13.2
W-11	0.35	8	1.82	13	0.08	0.42 [w]	7.77×10^{-8}	1.00×10^{-6}	0.51	1000	21.4	5.3
W-12	0.35	11.2	1.74	19	0.08	0.43 [w]	1.74×10^{-7}	1.00×10^{-6}	0.51	1461	32.1	10.5
W-13	0.35	16	1.67	20.5	0.08	0.44 [w]	4.01×10^{-7}	1.00×10^{-6}	0.51	1576	48.7	-
W-14	0.35	17.5	1.17	21	0.08	0.56[w]	1.56×10^{-6}	1.00×10^{-6}	0.51	1615	95.9	∞
W-15	0.35	8	1.9	16	0.08	0.41 [w]	6.86×10^{-8}	1.00×10^{-6}	0.51	1230	20.1	8.37
W-16	0.35	8	1.23	10	0.08	0.54 [w]	2.72×10^{-7}	1.00×10^{-6}	0.51	769	40.1	9.84
W-17	0.35	8.5	1.72	19	0.08	0.43 [w]	1.04×10^{-7}	1.00×10^{-6}	0.51	1461	24.8	16.1
W-18	0.35	8	1.46	11	0.08	0.48 [w]	1.53×10^{-7}	1.00×10^{-6}	0.51	846	30	15.4
W-19	0.35	4	1.65	8	0.08	0.45 [w]	2.60×10^{-8}	1.00×10^{-6}	0.51	615	12.4	-
W-20	0.35	8	1.82	13	0.08	0.42 [w]	7.77×10^{-8}	1.00×10^{-6}	0.51	1000	21.4	8.56
W-21	0.35	8	1.82	13	0.08	0.42 [w]	7.77×10^{-8}	1.00×10^{-6}	0.51	1000	21.4	11.3
W-22	0.35	11.2	1.74	19	0.08	0.43 [w]	1.74×10^{-7}	1.00×10^{-6}	0.51	1461	32.1	10.4
W-23	0.35	16	1.67	20.5	0.08	0.44 [w]	4.01×10^{-7}	1.00×10^{-6}	0.51	1576	48.7	9.55
W-24	0.35	17.5	1.17	21	0.08	0.56 [w]	1.56×10^{-6}	1.00×10^{-6}	0.51	1615	95.9	∞
W-25	0.35	8	1.9	16	0.08	0.41 [w]	6.86×10^{-8}	1.00×10^{-6}	0.51	1230	20.1	11.1
W-26	0.35	8	1.23	10	0.08	0.54 [w]	2.72×10^{-7}	1.00×10^{-6}	0.51	769	40.1	-
W-27	0.35	8.5	1.72	19	0.08	0.43 [w]	1.04×10^{-7}	1.00×10^{-6}	0.51	1461	24.8	12.5
W-28	0.35	8	1.46	11	0.08	0.48 [w]	1.53×10^{-7}	1.00×10^{-6}	0.51	846	30	-
W-29	0.35	4	1.65	8	0.08	0.45 [w]	2.60×10^{-8}	1.00×10^{-6}	0.51	615	12.4	4.07
W-30	0.35	8	1.82	13	0.08	0.42 [w]	7.77×10^{-8}	1.00×10^{-6}	0.51	1000	21.4	7.24

Table 2 (continued)

Test[γ]	d_{fs} (mm)	d_{ss} (mm)	σ_{ss}	k_s (mm)	u^* (ms^{-1})	φ	K (ms^{-1})	ν (ms^{-2})	Fr	Re^*	Re_K	Z_c $(cm)^{\varepsilon}$
G-1	0.4	8	1.38	9.5	0.05	0.33[w]	1.84×10^{-7}	1.00×10^{-6}	0.6	435	19.6	7.13
G-2	0.22	8	1.38	9.5	0.05	0.33[w]	1.84×10^{-7}	1.00×10^{-6}	0.6	435	19.6	7.02
G-3	0.21	8	1.38	9.5	0.05	0.33[w]	1.84×10^{-7}	1.00×10^{-6}	0.6	435	19.6	∞
G-4	0.12	8	1.38	9.5	0.05	0.33[w]	1.84×10^{-7}	1.00×10^{-6}	0.6	446	20.2	∞
G-5	0.22	8	1.38	9.5	0.05	0.33[w]	1.84×10^{-7}	1.00×10^{-6}	0.73	518	23.4	7.43
G-6	0.21	8	1.38	9.5	0.05	0.33[w]	1.84×10^{-7}	1.00×10^{-6}	0.73	518	23.4	∞
G-1	0.2	3.7	1.225	4.5	0.05	0.45	5.90×10^{-8}	1.00×10^{-6}	0.52	236	12.7	7.15
G-2	0.2	2.9	1.127	3.3	0.05	0.43	4.91×10^{-8}	1.00×10^{-6}	0.52	173	11.6	7.26
G-3	0.2	9.2	1.353	15	0.05	0.44	2.59×10^{-7}	1.00×10^{-6}	0.52	786	26.7	∞
G-4	0.2	7.6	1.4	10	0.05	0.51	1.58×10^{-7}	1.00×10^{-6}	0.52	524	20.8	∞
G-5	0.2	5.9	1.188	7.2	0.05	0.51	1.67×10^{-7}	1.00×10^{-6}	0.52	377	21.4	∞
G-1	0.63	7.6	1.4	10.1	0.05	0.33[w]	1.58×10^{-7}	1.00×10^{-6}	0.51	529	20.8	6.59
G-2	0.34	7.6	1.4	10.1	0.05	0.33[w]	1.58×10^{-7}	1.00×10^{-6}	0.51	529	20.8	7.92
K-1	0.3	35	1.15	40	0.12	0.4	1.22×10^{-6}	1.00×10^{-6}	0.55	4781	132	∞
K-2	0.3	35	1.15	40	0.05	0.4	1.22×10^{-6}	1.00×10^{-6}	0.27	2119	58.5	∞
K-3	0.3	35	1.15	40	0.09	0.4	1.22×10^{-6}	1.00×10^{-6}	0.45	3655	100.9	∞
K-4	0.3	35	1.15	40	0.12	0.4	1.22×10^{-6}	1.00×10^{-6}	0.55	4738	130.8	∞
K-5	0.3	35	1.15	40	0.05	0.4	1.22×10^{-6}	1.00×10^{-6}	0.26	2040	56.3	∞
K-6	0.3	35	1.15	40	0.09	0.4	1.22×10^{-6}	1.00×10^{-6}	0.45	3542	97.8	∞
K-7	0.3	35	1.15	40	0.12	0.4	1.22×10^{-6}	1.00×10^{-6}	0.56	4810	132.8	∞
K-8	0.3	35	1.15	40	0.12	0.4	1.22×10^{-6}	1.00×10^{-6}	0.56	4774	131.8	∞
K-9	0.3	35	1.15	40	0.09	0.4	1.22×10^{-6}	1.00×10^{-6}	0.45	3502	96.7	∞
K-10	0.3	35	1.15	40	0.11	0.4	1.22×10^{-6}	1.00×10^{-6}	0.57	4483	123.8	∞
K-11	0.3	35	1.15	40	0.05	0.4	1.22×10^{-6}	1.00×10^{-6}	0.22	1958	54.1	∞
K-12	0.3	35	1.15	40	0.08	0.4	1.22×10^{-6}	1.00×10^{-6}	0.44	3211	88.7	∞
K-13	0.3	35	1.15	40	0.11	0.4	1.22×10^{-6}	1.00×10^{-6}	0.55	4367	120.6	∞
K-14	0.3	35	1.15	40	0.05	0.4	1.22×10^{-6}	1.00×10^{-6}	0.24	1922	53.1	∞
K-15	0.3	35	1.15	40	0.08	0.4	1.22×10^{-6}	1.00×10^{-6}	0.46	3174	87.6	∞

Table 2 (continued)

Test[γ]	d_{fs} (mm)	d_{ss} (mm)	σ_{ss}	k_s (mm)	u^* (ms^{-1})	φ	K (ms^{-1})	ν (ms^{-2})	Fr	Re^*	Re_K	Z_c $(cm)^{\varepsilon}$
K-16	0.3	35	1.15	40	0.1	0.4	1.22×10^{-6}	1.00×10^{-6}	0.59	3917	108.1	∞
K-17	0.3	35	1.15	40	0.05	0.4	1.22×10^{-6}	1.00×10^{-6}	0.24	1936	53.4	∞
K-18	0.3	35	1.15	40	0.08	0.4	1.22×10^{-6}	1.00×10^{-6}	0.44	3301	91.1	∞
K-19	0.3	35	1.15	40	0.11	0.4	1.22×10^{-6}	1.00×10^{-6}	0.58	4248	117.3	∞
K-20	0.3	35	1.15	40	0.04	0.4	1.22×10^{-6}	1.00×10^{-6}	0.19	1714	47.3	∞
K-21	0.3	35	1.15	40	0.05	0.4	1.22×10^{-6}	1.00×10^{-6}	0.26	1994	55	∞
K-22	0.3	35	1.15	40	0.09	0.4	1.22×10^{-6}	1.00×10^{-6}	0.46	3461	95.6	∞
K-23	0.3	35	1.15	40	0.1	0.4	1.22×10^{-6}	1.00×10^{-6}	0.58	3940	108.8	∞
K-24	0.3	35	1.15	40	0.05	0.4	1.22×10^{-6}	1.00×10^{-6}	0.25	1816	50.1	∞
K-25	0.3	35	1.15	40	0.07	0.4	1.22×10^{-6}	1.00×10^{-6}	0.45	2920	80.6	∞
K-26	0.3	35	1.15	40	0.1	0.4	1.22×10^{-6}	1.00×10^{-6}	0.6	4130	114	∞
K-27	0.3	35	1.15	40	0.03	0.4	1.22×10^{-6}	1.00×10^{-6}	0.19	1389	38.4	∞
K-28	0.3	35	1.15	40	0.04	0.4	1.22×10^{-6}	1.00×10^{-6}	0.27	1789	49.4	∞
K-29	0.3	35	1.15	40	0.07	0.4	1.22×10^{-6}	1.00×10^{-6}	0.47	2822	77.9	∞
K-30	0.3	35	1.15	40	0.11	0.4	1.22×10^{-6}	1.00×10^{-6}	0.6	4235	116.9	∞

Table 3. Summary of data.

Study	d_{fs} (mm)	d_s (mm)	σ_{ss}	ν_o	ϕ	K (m/s)	u* (m/s)	Re*	Re_K	Z_c (cm) Measured	Z_c (cm) Impulse-Model
W-1	0.35	8.00	1.82	1.0E-06	0.43	7.77E-08	0.077	1000	21.4	7.6	9
W-2	0.35	11.20	1.74	1.0E-06	0.44	1.74E-07	0.077	1461	32.1	11.3	10.5
W-3	0.35	16.00	1.67	1.0E-06	0.56	4.01E-07	0.077	1576	48.7	10.23	12.5
W-4	0.35	17.50	1.17	1.0E-06	0.41	1.56E-06	0.077	1615	95.9	16.19	23
W-5	0.35	8.00	1.9	1.0E-06	0.54	6.86E-08	0.077	1230	20.1	10.39	8.5
W-6	0.35	8.00	1.23	1.0E-06	0.43	2.72E-07	0.077	769	40.1	17.62	17
W-7	0.35	8.50	1.72	1.0E-06	0.48	1.04E-07	0.077	1461	24.8	10.33	10
W-8	0.35	8.00	1.46	1.0E-06	0.45	1.53E-07	0.077	846	30.0	10.77	13
W-9	0.35	4.00	1.65	1.0E-06	0.42	2.6E-08	0.077	615	12.4	10.17	8
W-10	0.35	8.00	1.82	1.0E-06	0.42	7.77E-08	0.077	1000	21.4	13.17	9
W-11	0.35	8.00	1.82	1.0E-06	0.43	7.77E-08	0.077	1000	21.4	5.3	9
W-12	0.35	11.20	1.74	1.0E-06	0.44	1.74E-07	0.077	1461	32.1	10.46	10.5
W-14	0.35	17.50	1.17	1.0E-06	0.41	1.56E-06	0.077	1615	95.9	23.82	23
W-15	0.35	8.00	1.9	1.0E-06	0.54	6.86E-08	0.077	1230	20.1	8.37	8.5
W-16	0.35	8.00	1.23	1.0E-06	0.43	2.72E-07	0.077	769	40.1	9.84	17
W-17	0.35	8.50	1.72	1.0E-06	0.48	1.04E-07	0.077	1461	24.8	16.13	10
W-18	0.35	8.00	1.46	1.0E-06	0.45	1.53E-07	0.077	846	30.0	15.41	13
W-20	0.35	8.00	1.82	1.0E-06	0.42	7.77E-08	0.077	1000	21.4	8.56	9
W-21	0.35	8.00	1.82	1.0E-06	0.43	7.77E-08	0.077	1000	21.4	11.3	9
W-22	0.35	11.20	1.74	1.0E-06	0.44	1.74E-07	0.077	1461	32.1	10.39	10.5
W-23	0.35	16.00	1.67	1.0E-06	0.56	4.01E-07	0.077	1576	48.7	9.55	12.5
W-25	0.35	8.00	1.9	1.0E-06	0.54	6.86E-08	0.077	1230	20.1	11.12	8.5
W-27	0.35	8.50	1.72	1.0E-06	0.48	1.04E-07	0.077	1461	24.8	12.52	10
W-29	0.35	4.00	1.65	1.0E-06	0.42	2.6E-08	0.077	615	12.4	4.07	8

Table 3 (continued)

Study	d_{fs} (mm)	d_s (mm)	σ_{ss}	ν_o	ϕ	K (m/s)	u* (m/s)	Re*	Re_K	Z_c (cm) Measured	Z_c (cm) Impulse-Model
W-30	0.35	8.00	1.82	1.0E-06	0.35	7.77E-08	0.077	1000	21.4	7.24	9
DP-1	0.11	2.44	2.75	1.0E-06	0.35	3.15E-09	0.059	356	3.3	2.7	3.5
DP-2	0.11	2.44	2.75	1.0E-06	0.35	3.15E-09	0.057	342	3.2	2.7	3.5
DP-3	0.11	2.44	2.75	1.0E-06	0.35	3.15E-09	0.057	344	3.2	2.7	3.5
DP-4	0.11	2.44	2.75	1.0E-06	0.35	3.15E-09	0.057	344	3.2	2.7	3.5
DP-5	0.11	2.44	2.75	1.0E-06	0.35	3.15E-09	0.057	343	3.2	2.7	3.5
DP-6	0.11	2.44	2.75	1.0E-06	0.35	3.15E-09	0.057	343	3.2	2.7	3.5
DP-7	0.11	2.44	2.75	1.0E-06	0.35	3.15E-09	0.045	272	2.5	2.35	3
DP-8	0.11	2.44	2.75	1.0E-06	0.35	3.15E-09	0.046	274	2.6	2.35	3
DP-9	0.11	2.44	2.75	1.0E-06	0.35	3.15E-09	0.046	275	2.6	2.35	3
DP-10	0.11	2.44	2.75	1.0E-06	0.35	3.15E-09	0.046	277	2.6	2.35	3
DP-11	0.11	2.44	2.75	1.0E-06	0.35	3.15E-09	0.046	276	2.6	2.35	3
DP-12	0.11	2.44	2.75	1.0E-06	0.35	3.15E-09	0.046	276	2.6	2.35	3
DP-13	0.08	2.44	2.75	1.0E-06	0.35	3.15E-09	0.047	280	2.6	2.65	3
DP-14	0.08	2.44	2.75	1.0E-06	0.35	3.15E-09	0.047	280	2.6	2.65	3
DP-15	0.08	2.44	2.75	1.0E-06	0.35	3.15E-09	0.047	280	2.6	2.65	3
DP-16	0.08	2.44	2.75	1.0E-06	0.35	3.15E-09	0.047	280	2.6	2.65	3
DP-17	0.08	2.44	2.75	1.0E-06	0.35	3.15E-09	0.047	281	2.6	2.65	3
DP-18	0.08	2.44	2.75	1.0E-06	0.27	3.15E-09	0.047	281	2.6	2.65	3
DP-19	0.08	2.44	2.75	1.0E-06	0.27	3.15E-09	0.047	281	2.6	2.65	3
G-1	0.40	8.00	1.38	1.0E-06	0.33	1.84E-07	0.046	435	19.6	7.1288	5
G-2	0.22	8.00	1.38	1.0E-06	0.33	1.84E-07	0.046	435	19.6	7.0169	6
G-5	0.22	8.00	1.38	1.0E-06	0.33	2.9E-06	0.054	518	92.7	7.4282	7.5
G-1	0.20	3.70	1.22	1.0E-06	0.42	1.69E-08	0.052	236	68.1	7.15	7

Table 3 (continued)

Study	d_{fs} (mm)	d_s (mm)	σ_{ss}	ν_o	ϕ	K (m/s)	u* (m/s)	Re*	Re_K	Z_c (cm) Measured	Z_c (cm) Impulse-Model
G-2	0.20	2.90	1.13	1.0E-06	0.43	1.15-08	0.052	173	56.3	7.26	7
G-1	0.63	7.60	1.4	1.0E-06	0.33	2.51E-06	0.052	529	83.1	6.59	4.5
G-2	0.34	7.60	1.4	1.0E-06	0.33	2.51E-06	0.052	529	83.1	7.92	6
D-1	0.12	2.25	2.75	1.0E-06	0.34	2.68E-09	0.050	280	2.6	4.86	3

REFERENCES

Belcher, B.J. and Fox, J.F. (2011). "Outer scaling for open channel flow over a gravel bed." *Journal of Engineering Mechanics*, ASCE, 137(1): 40-46.

Beschta, R. L., and Jackson, W. L. (1979). "The intrusion of fine sediments into a stable Gravel bed."*Journal of the Fisheries Board of Canada*, 36(2), 204-210.

Duan, X., Wang, Z., Xu, M., and Zhang, K. (2009). "Effect of streambed sediment on benthic ecology." *International Journal of Sediment Research*,24(3), 325-338.

Bullied, W. J., Flerchinger, G. N., Bullock, P. R., & Van Acker, R. C. (2014)."Process Based modeling of temperature and water profiles in the seedling recruitment zone: Part I. model validation". *Agricultural and Forest Meteorology*,188, 89 103.

Carling, P. A. (1984). "Deposition of fine and coarse sand in an open-work gravel bed." *Canadian Journal of Fisheries and Aquatic Sciences*, 41(2), 263-270.

Carling, P. A., and Reader, N. A. (1982). "Structure, composition and bulk properties of Upland stream gravels." *Earth Surface Processes and Landforms*, 7(4), 349-365.

Chapuis, R. P., and Aubertin, M. (2003). "On the use of the Kozeny Carman equation to Predict 17 the hydraulic conductivity of soils." Canadian Geotechnical Journal, 40(3), 616-628.

Cho, G.C., Dodds J., and Santamarina J.C. (2006). "Particle shape effects on packing density, stiffness, and strength: natural and crushed sands." *Journal of Geotechnical and Geoenvironmental Engineering*, 591-602.

Cui, Y., Wooster, J. K., Baker, P. F., Dusterhoff, S. R., Sklar, L. S., & Dietrich, W. E. (2008). "Theory of fine sediment infiltration into immobile gravel bed." Journal of Hydraulic Engineering, 134(10), 1421-1429.

Dermisis, D., and Papanicolaou, A.N. (2014). "The effects of protruding rock boulders in regulating sediment intrusion within the hyporheic zone of mountain streams." *Journal of Mountain Science*.

Dexter, A. R., and Tanner, D. W. (1972). "Packing densities of mixtures of spheres with Log normal size distributions." *Nature*, 238(80), 31-32.

Dhamotharan, S., Shirazi, M. A., and Corvallis Environmental Research Laboratory. (1980). *Bedload transport in a model gravel stream*. University of Minnesota, St. Anthony Falls Hydraulic Laboratory.

Diplas, P., and Parker, G. (1985). "Deposition and removal of fines in gravel-bed

streams." *Dynamics of Gravel-bed rivers*, 313-329.

Einstein, H. A. (1968). "Deposition of suspended particles in a gravel bed." *Journal of Hydraulic Engineering,* 94(5), 1197-1205.

Ford, W.I. and Fox, J.F. (2014). "Model of particulate organic carbon transport in an 431 agriculturally impacted stream". Hydrological Processes, 28(3), 662-675.

Fries, J. S. (2007). "Predicting interfacial diffusion coefficients for fluxes across the Sediment water interface." *Journal of Hydraulic Engineering*, 133(3), 267-272.

Fries, J. S., and Taghon, G. L. (2010). "Particle fluxes into permeable sediments: Comparison of mechanisms mediating deposition." *Journal of Hydraulic Engineering*, 136(4), 214-221.

Fries, J. S., & Trowbridge, J. H. (2003). "Flume observations of enhanced fine-particle deposition to permeable sediment beds". *Limnology and oceanography*,48(2), 802-812.

Frostick, L. E., Lucas, P. M., & Reid, I. (1984). "The infiltration of fine matrices into coarse grained alluvial sediments and its implications for stratigraphical interpretation*". Journal of the Geological Society*, 141(6), 955-965.

Gambhir, M.L. (2004). "Stability analysis and design of structures." Springer.

Gibson, S., Abraham, D., Heath, R., and Schoellhamer, D. (2008). "Vertical gradational variability of fines deposited in a gravel framework." *Sedimentology*, 56(3), 661 676.

Gibson, S., Abraham, D., Heath, R., and Schoellhamer, D. (2010). "Bridging process Threshold for sediment infiltrating into a coarse substrate." *Journal of Geotechnical and Geoenvironmental Engineering*, 136(2), 402-406.

Gibson, S., Heath, R., Abraham, D., and Schoellhamer, D. (2011). "Visualization and analysis of temporal trends of sand infiltration into a gravel bed." *Water Resources Research*, 47(12).

Gupta, R. D. (1985). "Angularity of aggregate particles as a measure of their shape and Hydraulic resistance." *Institution of Civil Engineers Proceedings PCIEAT*, *79*.

Harvey, B. (2000). "Testing times for arches." In: Masonary bridges, viaducts and aqueducts, Ruddock, T., Ashgate Publishing, Aldershot, Hampshire, Great Britain.

Higashino, M., and Stefan, H. G. (2008). "Near-bed turbulence models: Significance for diffusional mass transfer at the sediment/water interface." *Journal of Hydraulic*

Research, *46*(3), 291-300.

Higashino, M., Clark, J. J., and Stefan, H. G. (2009). "Pore water flow due to near-bed turbulence and associated solute transfer in a stream or lake sediment bed." *Water resources research*, *45*(12).

Huettel, M., and Rusch, A. (2000). "Transport and degradation of phytoplankton in Permeable sediment." *Limnology and Oceanography*, 45(3), 534-549.

Huston, D., and Fox, J. (2014). "Clogging of fine sediment within gravel substrates: Dimensional analysis and macro-analysis of experiments in hydraulic flumes". *Journal of Hydraulic Engineering*.

Hutchinson, P. A., and Webster, I. T. (1998). "Solute uptake in aquatic sediments due to Current obstacle interactions." *Journal of Environmental Engineering*, 124(5), 419-426.

Komura, S. (1963). "Discussion of 'Sediment transportation mechanics: Introduction and properties of sediment.' " *J. Hydraul. Div., Am. Soc. Civ. Eng.*, 89(1), 263–266.

Krou, J. F., Fox, J. F, and Safferman, S. (2006) "Sediment separation in a fluidized bed unit for soil washing purposes." Journal of Environmental Engineering, ASCE 132(10): 1307-1313.

Kuhnle, R. A., Wren, D. G., Langendoen, E. J., & Rigby, J. R. (2013). "Sand transport over an immobile gravel substrate." Journal of Hydraulic Engineering,139(2), 167 176.

Latham, J. P., Munjiza, A., & Lu, Y. (2002)."On the prediction of void porosity and packing of rock particulates." *Powder Technology*, *125*(1), 10-27.

Lauck, T.E. (1991). "A simulation model for the infiltration of sediment into spawning Gravel." Master's Thesis. Humboldt State University. August.

Leonardson, R. (2010). "Exchange of fine sediments with gravel riverbeds." PhD Dissertation, California, Berkeley Univ., Berkeley, Ca.

Li, L., Barry, D. A., Cuiligan-Hensley, P. J., and Bajracharya, K. (1994). "Mass transfer in soils with local stratification of hydraulic conductivity." *Water Resources Research*, 30(11), 2891-2900.

Lisle, T. E. (1989). "Sediment transport and resulting deposition in spawning gravels, North coastal California". *Water resources research*, 25(6), 1303-1319.

McDowell-Boyer, L. M., Hunt, J. R., & Sitar, N. (1986). "Particle transport through porous media." *Water Resources Research*, 22(13), 1901-1921.

Nagaoka, H., and Ohgaki, S. (1990). “Mass transfer mechanism in a porous riverbed.” *Water Research*, *24*(4), 417-425.

O'Connor, B. L., and Harvey, J. W. (2008). “Scaling hyporheic exchange and its influence on biogeochemical reactions in aquatic ecosystems.” *Water Resources Research*, *44*(12).

Peronius, N., & Sweeting, T. J. (1985). “On the correlation of minimum porosity with Particle size distribution.” *Powder Technology*, 42(2), 113-121.

Pugnaloni, L. A., and Barker, G. C. (2004). “Structure and distribution of arches in shaken hard sphere deposits.” *Physica A: Statistical Mechanics and its Applications*, *337*(3), 428-442.

Reidenbach, M. A., Limm, M., Hondzo, M., and Stacey, M. T. (2010). “Effects of bed Roughness on boundary layer mixing and mass flux across the sediment-water interface.” *Water Resources Research*, 46(7).

Rosgen, Dave. *Applied River Morphology*. Pagosa Springs: Wildland Hydrology. Print

Ruff, J. F., and Gelhar, L. W. (1972). “Turbulent shear flow in porous boundary.” *J. Eng. Mech*, *98*, 975.

Sakthivadivel, R., and Einstein, H. A. (1970). “Clogging of porous column of spheres by 457 sediment.” Journal of the Hydraulics Division, 96(2), 461-472.

Shimizu, Y., Tsujimoto, T., and Nakagawa, H. (1990). “Experiment and macroscopic Modelling of flow in highly permeable porous medium under free-surface flow.” *J. Hydrosci. Hydraul. Eng*, *8*(1), 69-78.

Simitses, G.J. and Hodges, D.H. (2005). “Fundamentals of structural stability.” Butterworth Heinemann, pages 333-336.

Sohn, H. Y., and Moreland, C. (1968). “The effect of particle size distribution on packing density.” *The Canadian Journal of Chemical Engineering*, 46(3), 162-167.

Suttle, K. B., Power, M. E., Levine, J. M., and McNeely, C. (2004). “How fine sediment In riverbeds impairs growth and survival of juvenile salmonids.” *Ecological Applications*, *14*(4), 969-974.

Valdes, Julio R., and Santamarina, J. C. (2006)."Particle clogging in radial flow: Microscale mechanisms." *SPE Journal-Richardson,*11(2), 193.

Valdes, J. R., and Santamarina, J. C. (2008). “Clogging: bridge formation and vibration Based destabilization.” *Canadian Geotechnical Journal*, *45*(2), 177-184.

Wakeman, R. J. (1975). “Packing densities of particles with log-normal size

distributions." *Powder technology*, 11(3), 297-299.

Wood, P.J. and Armitage, P.D. (1997). "Biological effects of fine sediment in the lotic 463 environment." Environmental Management 21(2): 203–217

Wooster, J. K., Dusterhoff, S. R., Cui, Y., Sklar, L. S., Dietrich, W. E., and Malko, M. (2008). "Sediment supply and relative size distribution effects on fine sediment infiltration into immobile gravels." *Water Resources Research*, 44(3).

Wu, F.C., and Huang H.T. (2000). "Hydraulic resistance induced by deposition of sediment in porous medium." *Journal of Hydraulic Engineering*, 126, 547-551.

Wu, W., and Wang, S. S. (2006). "Formulas for sediment porosity and settling velocity." *Journal of Hydraulic Engineering*, 132(8), 858-862.

Youd, T. L. (1973). "Factors controlling maximum and minimum densities of sands." In *Evaluation of Relative Density and Its Role in Geotechnical Projects Involving Cohesionless Soils: A Symposium Presented at the Seventy-fifth Annual Meeting American Society for Testing and Materials (ASTM)* (Vol. 523, p. 98). ASTM International.

Zou, R. P., and Yu, A. B. (1996). "Evaluation of the packing characteristics of mono sized non spherical particles." *Powder Technology*, 88(1), 71-79.

Vita - Davis Huston

Education:

- BS in Civil Engineering, University of Kentucky, August 2008 – December 2012
  Minor: Mathematics
  GPA: 3.859
  Summa Cum Laude

- MS in Civil Engineering, University of Kentucky, January 2013 – December 2014

Professional Positions:

- Project Engineer, Stantec Consulting, January 2014 - Present

Awards and Honors:

- C. Michael Garver Scholarship, 2012
- Undergraduate Research Grant, 2012
- University Scholars Program, 2012
- Outstanding University Scholar Award, 2013
- Raymond Fellowship, 2013
- Chi Epsilon Member